

Determining the geometry of noncircular gears for given transmission function

Uwe Bäsel

Abstract

A pair of noncircular gears can be used to generate a strictly increasing continuous function $\psi(\varphi)$ whose derivative $\psi'(\varphi) = d\psi(\varphi)/d\varphi > 0$ is $2\pi/n$ -periodic, where φ and $\gamma = \psi(\varphi)$ are the angles of the opposite rotation directions of the drive gear and the driven gear, respectively, and $n \in \mathbb{N} \setminus \{0\}$. In this paper, we determine the geometry of both gears for given transmission function $\psi(\varphi)$ when manufacturing with a rack-cutter having fillets. All occurring functions are consistently derived as functions of the drive angle φ and the function ψ . Throughout the paper, methods of complex algebra, including an external product, are used. An effective algorithm for the calculation of the tooth geometries – in general every tooth has its own shape – is presented which limits the required numerical integrations to a minimum. Simple criteria are developed for checking each tooth flank for undercut. The base curves of both gears are derived, and it is shown that the tooth flanks are indeed the involutes of the corresponding base curve. All formulas for both gears are ready to use.

2010 Mathematics Subject Classification: 53A04, 53A17, 51N20, 15A75

Keywords: Noncircular gears, involute gears, transmission function, envelope, undercut, evolute, exterior product

1 Introduction

Toothed gears are used in many technical systems. The most important and most frequently used type of gearing nowadays is the involute gearing dating back to Leonhard Euler (1765/67) [4]. Involute gears have the advantages that they are easy to manufacture – hence cost-effective – and ensure a constant transmission ratio even if the centre distance is not exactly maintained. Furthermore, they have good mating properties. The working flanks of the teeth are the involutes of a circle, which is called base circle. (Clearly, the base circle is the evolute of these involutes.) For the manufacture of involute gears, straight flank tools are often used, for example so-called rack-cutters. (The profile of such a rack-cutter is shown in Fig. 2.2.)

In addition to the well-known circular gears for constant transmission ratios, there are also noncircular gears for non-constant transmission ratios, which also play an important role (see Litvin and Fuentes [7, Chapter 12], Litvin et al. [10]). They are often used for the generation of motions with periodic transmission ratio, such as those required in printing, packaging, textile and many other types of machines. Elliptical gears (see e.g. Wunderlich [15, pp. 233-235, 242-244], Chen and Tsay [2], Litvin and Fuentes [7, pp. 324-327], Litvin et al. [9], [10, pp. 40-52]), for example, can be applied for this purpose. However, these only provide suitable rotational motions to a limited extent (see Fig. 172 in [15, p. 235]). It is better to specify the required motion (transmission function) and dimension the gear drive so that it realizes this motion. Tsay and Fong [14] use Fourier series approximation of centrodes and gear ratios in order to derive the tooth profiles of noncircular gears (see e.g. Example 3 on pp. 567-568). The determination of the centrodes for given transmission functions is investigated in [8], especially in Section 4. Qiu and Deng [13] calculate the tooth profile for given transmission function when manufacturing

with rack-cutter, but only for the left sides of the gear tooth spaces. The calculations require case distinctions that are not discussed.

In this paper, we calculate the complete tooth profiles of the drive and the driven gear when manufacturing with a rack-cutter having fillets. All calculations are based on the transmission function, and so all functions are consistently related to the rotation angle φ of the drive gear. We use complex-valued functions of the real variable φ (see e.g. Wunderlich [15], Müller [12], Luck and Modler [11], Laczik, Zentay, and Horváth [6]). This allows a very simple and transparent derivation of the results. Undercut conditions are obtained for both gears. Equations for the base curves are derived. A detailed algorithm summarizes all necessary calculation steps.

The paper is organized as follows:

- In Section 2 we introduce some basic notation and foundations that we will use throughout the paper.
- In Section 3 we derive a parametric equation for the flank curves of the drive gear in two different ways: 1) by obtaining the flank curves as envelopes of the rack-cutter flanks, applying an exterior product for complex numbers, 2) using the instantaneous centre of velocity of drive gear and rack-cutter. Furthermore, we derive a parametric equation for the fillet curves.
- Section 4 provides the calculations for the driven gear analogous to those of Section 3.
- In Section 5, undercut conditions are derived for the drive and the driven gear.
- Parametric equations for the base curves are derived in Section 6. As a by-product the curvatures of the flank curves are obtained.
- Section 7 is a detailed algorithm for the complete profiles of both gears.
- Section 8 gives a practical example.
- Calculation rules for the exterior product are to be found in Appendix A, a list of the used formula symbols in Appendix B.

2 Preliminaries

We denote by φ the rotation angle of the drive gear, and by γ the rotation angle of the driven gear. Let

$$\psi: [0, 2\pi] \rightarrow \mathbb{R}, \quad \varphi \mapsto \psi(\varphi) \quad (2.1)$$

be a strictly increasing continuous function whose derivative

$$\psi'(\varphi) = \frac{d\psi(\varphi)}{d\varphi} > 0 \quad (2.2)$$

is $2\pi/n$ -periodic, $n \in \mathbb{N} \setminus \{0\}$. Our aim is to determine drive and driven gear in such a way that the relationship between φ and γ is given by

$$\gamma = \psi(\varphi). \quad (2.3)$$

The function ψ is called *transmission function*.

Let $\varphi^*(t)$ denote the rotation angle of the drive gear as function of time t . Then, the rotation angle of the driven gear as time function is given by

$$\psi^*(t) := \psi(\varphi^*(t)). \quad (2.4)$$

With $\varphi = \varphi^*(t)$ we get

$$\frac{d\psi^*(t)}{dt} = \frac{d\psi(\varphi^*(t))}{d\varphi} = \frac{d\psi}{d\varphi}(\varphi^*(t)) \cdot \frac{d\varphi^*(t)}{dt} \quad (2.5)$$

From (2.5) with (2.2) it follows that

$$\psi'(\varphi^*(t)) = \frac{d\psi}{d\varphi}(\varphi^*(t)) = \frac{\dot{\psi}^*(t)}{\dot{\varphi}^*(t)}, \quad (2.6)$$

where the over-dot indicates time derivatives. So one sees that ψ' is the ratio of the angular velocities $\dot{\psi}^*$ and $\dot{\varphi}^*$ of driven gear and drive gear, respectively.

Let P be the instantaneous center of relative rotation of drive and driven gear (see Fig. 2.1). With the distance $a = |\overline{O_1O_2}|$ between the pivot points O_1 and O_2 we get

$$r(\varphi) + R(\varphi) = a \quad \text{and} \quad \psi'(\varphi) = \frac{|\overline{O_1P}|}{|\overline{O_2P}|} = \frac{r(\varphi)}{R(\varphi)}.$$

It follows that

$$r(\varphi) = \frac{a\psi'(\varphi)}{1 + \psi'(\varphi)} \quad \text{and} \quad R(\varphi) = \frac{a}{1 + \psi'(\varphi)}. \quad (2.7)$$

The instantaneous center P is in the rotating x, y -system given by $X_P(\varphi) = r(\varphi) e^{-i\varphi}$, hence here the path of P is the curve (centrode of the drive gear)

$$X_P: [0, 2\pi] \rightarrow \mathbb{C}, \quad \varphi \mapsto X_P(\varphi) = r(\varphi) e^{-i\varphi}. \quad (2.8)$$

In the rotating ξ, η -system, the path of P is the curve (centrode of the driven gear)

$$\Xi_P: [0, 2\pi] \rightarrow \mathbb{C}, \quad \varphi \mapsto \Xi_P(\varphi) = -R(\varphi) e^{i\psi(\varphi)}. \quad (2.9)$$

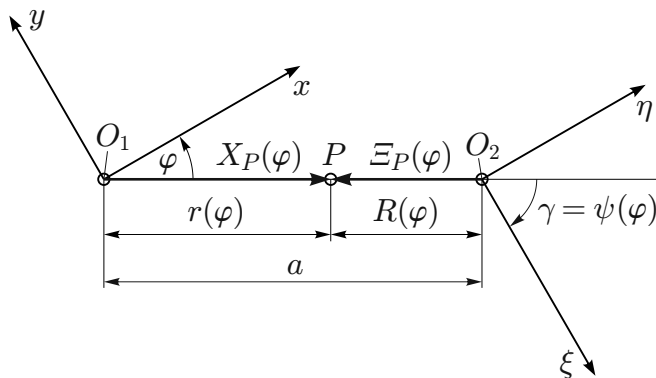


Fig. 2.1: Generation of the centrodes X_P and Ξ_P

The arc length of X_P between the points $X_P(\varphi_0)$ and $X_P(\varphi_1)$ is given by

$$s(\varphi_0, \varphi_1) = \int_{\varphi_0}^{\varphi_1} |X'_P(\varphi)| d\varphi, \quad (2.10)$$

where $X'_P(\varphi) = \frac{dX_P(\varphi)}{d\varphi}$ is the tangent vector of X_P at point $X_P(\varphi)$ (momentary contact point of X_P and Ξ_P). From (2.8) one gets

$$X'_P(\varphi) = r'(\varphi)e^{-i\varphi} - r(\varphi)ie^{-i\varphi} = (r'(\varphi) - ir(\varphi)) e^{-i\varphi},$$

hence

$$\begin{aligned} |X'_P(\varphi)| &= |(r'(\varphi) - ir(\varphi)) e^{-i\varphi}| = |r'(\varphi) - ir(\varphi)| |e^{-i\varphi}| \\ &= |r'(\varphi) - ir(\varphi)| = \sqrt{r'^2(\varphi) + r^2(\varphi)}. \end{aligned}$$

From $r(\varphi)$ in (2.7) we find

$$r'(\varphi) = \frac{a\psi''(\varphi)}{(1 + \psi'(\varphi))^2}.$$

It follows that

$$X'_P(\varphi) = \left(\frac{a\psi''(\varphi)}{(1 + \psi'(\varphi))^2} - \frac{ai\psi'(\varphi)}{1 + \psi'(\varphi)} \right) e^{-i\varphi} = \frac{a\psi''(\varphi) - ai\psi'(\varphi)(1 + \psi'(\varphi))}{(1 + \psi'(\varphi))^2} e^{-i\varphi}$$

and

$$|X'_P(\varphi)| = \sqrt{\frac{a^2\psi''^2(\varphi)}{(1 + \psi'(\varphi))^4} + \frac{a^2\psi'^2(\varphi)}{(1 + \psi'(\varphi))^2}} = \frac{aw(\varphi)}{(1 + \psi'(\varphi))^2} \quad (2.11)$$

with

$$w(\varphi) := \sqrt{\psi''^2(\varphi) + \psi'^2(\varphi)(1 + \psi'(\varphi))^2}. \quad (2.12)$$

So we have found

$$s(\varphi_0, \varphi_1) = aI(\varphi_0, \varphi_1),$$

where

$$I(\varphi_0, \varphi_1) := \int_{\varphi_0}^{\varphi_1} \frac{w(\varphi)}{(1 + \psi'(\varphi))^2} d\varphi. \quad (2.13)$$

The perimeter u of X_P ist given by $u = aI(0, 2\pi)$. We have

$$u = aI(0, 2\pi) = z_1 p = z_1 \pi m,$$

where z_1 is the number of teeth of the drive gear, p the tooth pitch and m the module (see Fig. 2.2), hence

$$a = \frac{z_1 \pi m}{I(0, 2\pi)}. \quad (2.14)$$

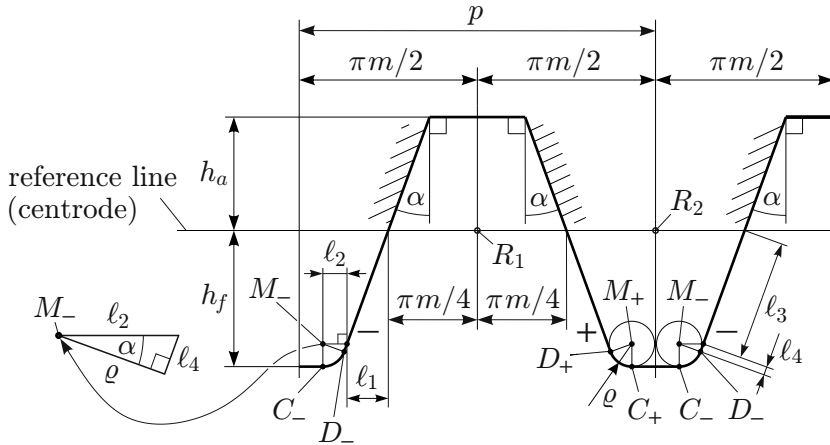


Fig. 2.2: Reference profile of the rack-cutter

Fig. 2.3 is crucial for all further considerations and calculations. The reference line (centrode) of the rack-cutter is always tangent to the centrodes X_P and Ξ_P at the instantaneous rotation center P . During the rotations of X_P and Ξ_P about O_1 and O_2 , respectively, the reference line is shifted between X_P and Ξ_P , where it generally rotates around P . Rigidly connected to the reference line are the two flanks marked with “+” and “-”. (Note that P in general is not in the middle between both flanks.) The relative motion between one of the centrodes and the reference line is a pure

rolling. The flanks “+” and “-” produce the corresponding flank curves “+” and “-”, respectively, of tooth k of the drive gear ($X_{F,k,\pm}$ in Fig. 3.2) and tooth space k of the driven gear.

Convention: In order to abbreviate the text, the following convention will be used throughout the paper. In formula symbols and formulas that contain “ \pm ” and sometimes also “ \mp ”, the upper sign is for the “+”-flank and the lower sign for the “-”-flank. Example: The sentences “The point M_{\pm} in Fig. 2.2 generates the curve $X_{M,k,\pm}$ in Fig. 3.2.” and “The points M_{\pm} in Fig. 2.2 generate the curves $X_{M,k,\pm}$ in Fig. 3.2.” are abbreviations for the sentence “The points M_+ and M_- in Fig. 2.2 generate the curves $X_{M,k,+}$ and $X_{M,k,-}$, respectively, in Fig. 3.2.” (Since Fig. 3.2 shows the curves for a tooth of the drive gear, the point M_- is the left one in Fig. 2.2.)

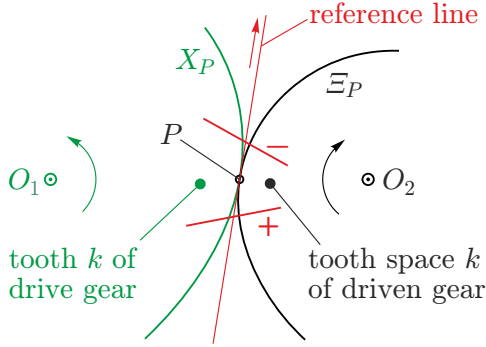


Fig. 2.3: Definition of the flanks “+” and “-”

3 Drive gear

The tangent unit vector T at point $X_P(\varphi)$ of X_P (see Fig. 3.1) is given by

$$T(\varphi) := \frac{X'_P(\varphi)}{|X'_P(\varphi)|} = \frac{\psi''(\varphi) - i\psi'(\varphi)(1 + \psi'(\varphi))}{w(\varphi)} e^{-i\varphi}. \quad (3.1)$$

Splitting (3.1) into real and imaginary part gives

$$\left. \begin{aligned} t_x(\varphi) &:= \operatorname{Re} T(\varphi) = \frac{\psi''(\varphi) \cos \varphi - \psi'(\varphi)(1 + \psi'(\varphi)) \sin \varphi}{w(\varphi)}, \\ t_y(\varphi) &:= \operatorname{Im} T(\varphi) = -\frac{\psi''(\varphi) \sin \varphi + \psi'(\varphi)(1 + \psi'(\varphi)) \cos \varphi}{w(\varphi)}. \end{aligned} \right\} \quad (3.2)$$

We denote the value of φ in the middle of the tooth k to be generated by $\chi(k)$, $k = 1, \dots, z_1$. One gets these values – in general numerically – from

$$aI(0, \chi(k)) = (k - 1)\pi m \quad (3.3)$$

with $I(\cdot, \cdot)$ according to (2.13), and a according to (2.14).

Now we determine a parametric equation for the rack-cutter flank line $X_{W,k,\pm}$ (see Fig. 3.1) that generates tooth flank curve $X_{F,k,\pm}$, $k = 1, 2, \dots, z_1$ (see Fig. 3.2). If $\varphi = \chi(k)$, then the point R_1 of the rack-cutter coincides with the point $X_P(\chi(k))$ of the centre X_P (see Fig. 3.1). The vectors $T(\varphi)$ and $\overrightarrow{X_P(\varphi)R_1}$ point into the same direction if $I(\chi(k), \varphi) < 0$, which is not the case in Fig. 3.1. The signed arc length between the points $X_P(\chi(k))$ and $X_P(\varphi)$ (= signed distance between R_1 and $X_P(\varphi)$) is equal to $aI(\chi(k), \varphi)$. The signed distances $\lambda_{k,+}(\varphi)$ and $\lambda_{k,-}(\varphi)$ are given by

$$\lambda_{k,\pm}(\varphi) := \pm \frac{\pi m}{4} - aI(\chi(k), \varphi). \quad (3.4)$$

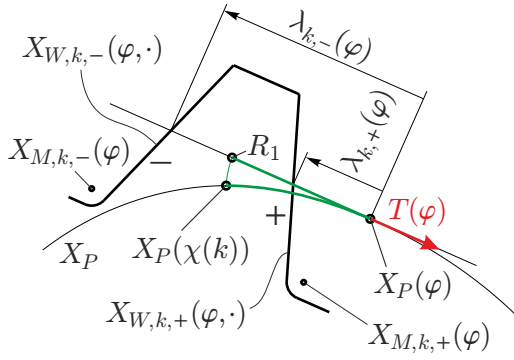


Fig. 3.1: Motion of the rack-cutter during the generation of tooth k

$\lambda_{k,\pm}(\varphi) > 0$ indicates that $T(\varphi)$ and the arrow of $\lambda_{k,\pm}(\varphi)$ have the same direction. So we have the following parametric equation for the rack-cutter flank line $X_{W,k,\pm}$

$$\begin{aligned} X_{W,k,\pm}(\varphi, \mu) &= X_P(\varphi) + \lambda_{k,\pm}(\varphi) T(\varphi) + \mu T(\varphi) e^{i(\frac{\pi}{2} \pm \alpha)} \\ &= X_P(\varphi) + \lambda_{k,\pm}(\varphi) T(\varphi) + \mu T(\varphi) i e^{\pm i\alpha} \\ &= X_P(\varphi) + (\lambda_{k,\pm}(\varphi) + \mu i e^{\pm i\alpha}) T(\varphi), \quad \mu \in \mathbb{R}. \end{aligned} \quad (3.5)$$

Splitting (3.5) into real and imaginary part gives

$$\left. \begin{aligned} x_{W,k,\pm}(\varphi, \mu) &= r(\varphi) \cos(\varphi) + \lambda_{k,\pm}(\varphi) t_x(\varphi) + \mu (\mp t_x(\varphi) \sin \alpha - t_y(\varphi) \cos \alpha), \\ y_{W,k,\pm}(\varphi, \mu) &= -r(\varphi) \sin(\varphi) + \lambda_{k,\pm}(\varphi) t_y(\varphi) + \mu (\mp t_y(\varphi) \sin \alpha + t_x(\varphi) \cos \alpha). \end{aligned} \right\} \quad (3.6)$$

Now, we determine a parametric equation of the tooth flank curves $X_{F,k,\pm}$.

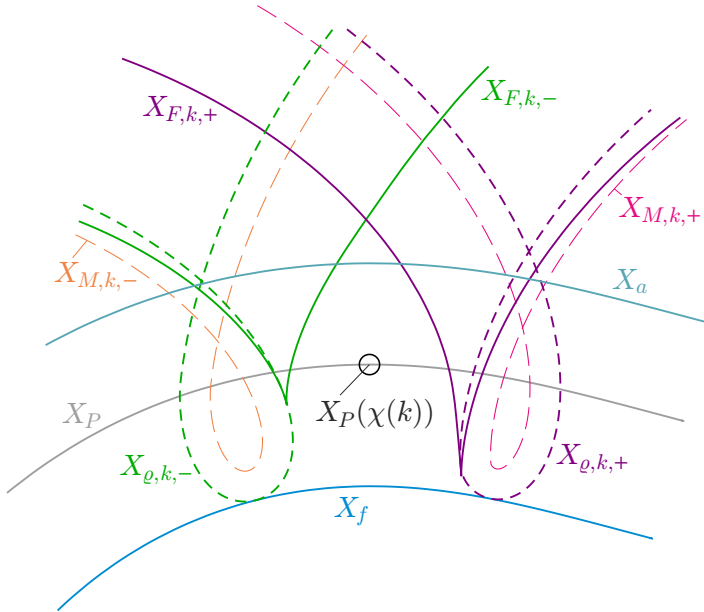


Fig. 3.2: Curves for tooth k (example):

$X_{F,k,\pm}$ flank curves,
 $X_{M,k,\pm}$ curves of M_{\pm}
 (see Fig. 2.2),
 $X_{\rho,k,\pm}$ fillet curves,
 X_P centre,
 X_a addendum curve,
 X_f dedendum curve

Theorem 3.1. A parametric equation of the flank curves $X_{F,k,\pm}$ (see Fig. 3.2) of tooth k , $k = 1, 2, \dots, z_1$, of the drive gear is given by

$$X_{F,k,\pm}(\varphi) = X_P(\varphi) + \lambda_{k,\pm}(\varphi) T(\varphi) e^{\pm i\alpha} \cos \alpha, \quad (3.7)$$

where

$$X_P(\varphi) = r(\varphi) e^{-i\varphi}, \quad T(\varphi) = \frac{\psi''(\varphi) - i\psi'(\varphi)(1 + \psi'(\varphi))}{w(\varphi)} e^{-i\varphi},$$

$$\lambda_{k,\pm}(\varphi) = \pm \frac{\pi m}{4} - a \int_{\chi(k)}^{\varphi} \frac{w(\phi)}{(1 + \psi'(\phi))^2} d\phi.$$

with

$$r(\varphi) = \frac{\alpha\psi'(\varphi)}{1 + \psi'(\varphi)}, \quad w(\varphi) = \sqrt{\psi'^2(\varphi) + \psi'^2(\varphi) (1 + \psi'(\varphi))^2},$$

and $\chi(k)$ according to (3.3).

Proof. Choosing two points (complex numbers) $A = A(\varphi)$, $B = B(\varphi)$ of the rack-cutter flank line $X_{W,k,+}(\varphi, \cdot)$ or $X_{W,k,-}(\varphi, \cdot)$, the equation of this line can be written as

$$[A(\varphi) - B(\varphi), X] = [A(\varphi), B(\varphi)] \quad (3.8)$$

(cp. (A.7)). A tooth flank curve is the envelope (see e.g. Baule [1, pp. 94-98]) of the family (3.8) of cutter flank lines with φ varying in a suitable interval. The equation of the envelope can be obtained from the linear equation system

$$\left. \begin{aligned} [A - B, X] &= [A, B], \\ [(A - B)', X] &= [A, B]' \end{aligned} \right\}$$

which, according to (A.1), can be written as

$$\left. \begin{aligned} \overline{(A - B)} X - (A - B) \overline{X} &= 2i[A, B], \\ \overline{(A - B)'} X - (A - B)' \overline{X} &= 2i[A, B]'. \end{aligned} \right\} \quad (3.9)$$

The solution of (3.9) is given by

$$\begin{aligned} X &= \frac{\begin{vmatrix} 2i[A, B] & -(A - B) \\ 2i[A, B]' & -(A - B)' \end{vmatrix}}{\begin{vmatrix} \overline{(A - B)} & -(A - B) \\ \overline{(A - B)'} & -(A - B)' \end{vmatrix}} = 2i \frac{[A, B] (A - B)' - [A, B]' (A - B)}{(\overline{(A - B)} (A - B)' - (A - B) \overline{(A - B)'})} \\ &= \frac{[A, B] (A - B)' - [A, B]' (A - B)}{[A - B, (A - B)']}. \end{aligned} \quad (3.10)$$

Let us choose

$$\begin{aligned} A &= A(\varphi) := X_{W,k,\pm}(\varphi, 1) = X_P(\varphi) + \lambda_{k,\pm}(\varphi) T(\varphi) + i e^{\pm i\alpha} T(\varphi), \\ B &= B(\varphi) := X_{W,k,\pm}(\varphi, 0) = X_P(\varphi) + \lambda_{k,\pm}(\varphi) T(\varphi), \end{aligned}$$

then we have

$$A - B = i e^{\pm i\alpha} T(\varphi), \quad (A - B)' = i e^{\pm i\alpha} T'(\varphi).$$

From (A.5), it follows that

$$\begin{aligned} [A - B, (A - B)'] &= [i e^{\pm i\alpha} T(\varphi), i e^{\pm i\alpha} T'(\varphi)] = i e^{\pm i\alpha} \overline{i e^{\pm i\alpha}} [T(\varphi), T'(\varphi)] \\ &= e^{\pm i\alpha} e^{\mp i\alpha} [T(\varphi), T'(\varphi)] = [T(\varphi), T'(\varphi)]. \end{aligned}$$

In the following we respectively write X_P , T , λ , w and ψ instead of $X_P(\varphi)$, $T(\varphi)$, $\lambda_{k,\pm}(\varphi)$, $w(\varphi)$ and $\psi(\varphi)$. Applying (A.2), (A.3), (A.4) and (A.5), we obtain

$$\begin{aligned} [A, B] &= [X_P + \lambda T + i e^{\pm i\alpha} T, X_P + \lambda T] \\ &= [X_P + \lambda T, X_P + \lambda T] + [i e^{\pm i\alpha} T, X_P + \lambda T] \\ &= [i e^{\pm i\alpha} T, X_P] + \lambda [i e^{\pm i\alpha} T, T] = [i e^{\pm i\alpha} T, X_P] + \lambda T \overline{T} [i e^{\pm i\alpha}, 1] \\ &= [i e^{\pm i\alpha} T, X_P] - \lambda [1, i e^{\pm i\alpha}] = [i e^{\pm i\alpha} T, X_P] - \lambda \operatorname{Im}(i e^{\pm i\alpha}) \\ &= [i e^{\pm i\alpha} T, X_P] - \lambda \cos \alpha, \end{aligned}$$

hence, with (3.1), (A.2), (A.3), (A.4), (A.5) and (A.6),

$$\begin{aligned}
[A, B]' &= [i e^{\pm i\alpha} T', X_P] + [i e^{\pm i\alpha} T, X'_P] - \lambda' \cos \alpha \\
&= [i e^{\pm i\alpha} T', X_P] + [i e^{\pm i\alpha} T, |X'_P| T] - \lambda' \cos \alpha \\
&= [i e^{\pm i\alpha} T', X_P] + |X'_P| T \bar{T} [i e^{\pm i\alpha}, 1] - \lambda' \cos \alpha \\
&= [i e^{\pm i\alpha} T', X_P] - |X'_P| [1, i e^{\pm i\alpha}] - \lambda' \cos \alpha \\
&= [i e^{\pm i\alpha} T', X_P] - |X'_P| \cos \alpha - \lambda' \cos \alpha.
\end{aligned} \tag{3.11}$$

For the derivative of $\lambda_{k,\pm}(\varphi)$ from (3.4) we find

$$\lambda'_{k,\pm}(\varphi) = \frac{d}{d\varphi} \left(\pm \frac{\pi m}{4} - a \int_{\chi(k)}^{\varphi} \frac{w(\phi)}{(1 + \psi'(\phi))^2} d\phi \right) = -\frac{aw(\varphi)}{(1 + \psi'(\varphi))^2}. \tag{3.12}$$

Comparing (3.12) with (2.11) one sees that

$$\lambda'_{k,\pm}(\varphi) = -|X'_P(\varphi)| \tag{3.13}$$

which simplifies (3.11) to

$$[A, B]' = [i e^{\pm i\alpha} T', X_P].$$

Now, (3.10) may be written as

$$X = \frac{([i e^{\pm i\alpha} T, X_P] - \lambda \cos \alpha) T' - [i e^{\pm i\alpha} T', X_P] T}{[T, T']} i e^{\pm i\alpha}. \tag{3.14}$$

It is necessary to determine the derivative of $T(\varphi)$. We write (3.1) as

$$T w e^{i\varphi} = \psi'' - i\psi' - i\psi'^2,$$

and get

$$T' w e^{i\varphi} + T w' e^{i\varphi} + T w i e^{i\varphi} = \psi^{(3)} - i\psi'' - 2i\psi'\psi'',$$

hence

$$\begin{aligned}
T' &= \frac{(\psi^{(3)} - i\psi'' - 2i\psi'\psi'') e^{-i\varphi} - T w' - iT w}{w} \\
&= \frac{T}{w^2} \left(w \frac{\psi^{(3)} - i\psi'' - 2i\psi'\psi''}{T} e^{-i\varphi} - w w' - iw^2 \right) \\
&= \frac{T}{w^2} \left(w^2 \frac{\psi^{(3)} - i\psi'' - 2i\psi'\psi''}{\psi'' - i\psi'(1 + \psi')} - w w' - iw^2 \right) \\
&= \frac{T}{w^2} \left(w^2 \frac{\psi^{(3)} - i\psi'' - 2i\psi'\psi''}{\psi'' - i\psi'(1 + \psi')} \frac{\psi'' + i\psi'(1 + \psi')}{\psi'' + i\psi'(1 + \psi')} - w w' - iw^2 \right) \\
&= \frac{T}{w^2} \left[(\psi^{(3)} - i\psi'' - 2i\psi'\psi'') (\psi'' + i\psi' + i\psi'^2) - w w' - iw^2 \right].
\end{aligned} \tag{3.15}$$

With

$$w' = \frac{\psi'' (\psi' + 3\psi'^2 + 2\psi'^3 + \psi^{(3)})}{w},$$

(3.15) becomes

$$\begin{aligned}
T' &= T w^{-2} \left[(\psi'' + i\psi' + i\psi'^2) (\psi^{(3)} - i\psi'' - 2i\psi'\psi'') - \psi'' (\psi' + 3\psi'^2 + 2\psi'^3 + \psi^{(3)}) \right. \\
&\quad \left. - i (\psi''^2 + \psi'^2 + 2\psi'^3 + \psi'^4) \right]
\end{aligned}$$

$$\begin{aligned}
&= T w^{-2} \left(\psi'' \psi^{(3)} - i \psi''^2 - 2i \psi' \psi''^2 + i \psi' \psi^{(3)} + \psi' \psi'' + 2\psi'^2 \psi'' + i \psi'^2 \psi^{(3)} + \psi'^2 \psi'' + 2\psi'^3 \psi'' \right. \\
&\quad \left. - \psi'' \psi' - 3\psi'' \psi'^2 - 2\psi'' \psi'^3 - \psi'' \psi^{(3)} - i \psi''^2 - i \psi'^2 - 2i \psi'^3 - i \psi'^4 \right) \\
&= iT w^{-2} \left(\psi' \psi^{(3)} + \psi'^2 \psi^{(3)} - \psi'^2 - 2\psi'^3 - \psi'^4 - 2\psi''^2 - 2\psi' \psi''^2 \right) \\
&= iT w^{-2} \left[(1 + \psi') \psi' \psi^{(3)} - (1 + \psi')^2 \psi'^2 - 2(1 + \psi') \psi''^2 \right] \\
&= iT w^{-2} (1 + \psi') \left[\psi' \left(\psi^{(3)} - \psi' - \psi'^2 \right) - 2\psi''^2 \right].
\end{aligned}$$

So, with the function

$$\begin{aligned}
h &: [0, 2\pi] \rightarrow \mathbb{R} \\
\varphi &\mapsto h(\varphi) := \frac{(1 + \psi'(\varphi)) [\psi'(\varphi) (\psi^{(3)}(\varphi) - \psi'(\varphi) - \psi'^2(\varphi)) - 2\psi''^2(\varphi)]}{w^2(\varphi)}, \tag{3.16}
\end{aligned}$$

we have found

$$T'(\varphi) = i h(\varphi) T(\varphi). \tag{3.17}$$

Applying (3.17), we get

$$[T, T'] = [T, ihT] = h [T, iT] = h T \bar{T} [1, i] = h$$

and

$$[i e^{\pm i\alpha} T', X_P] = [i e^{\pm i\alpha} ihT, X_P] = [-e^{\pm i\alpha} hT, X_P] = -h [e^{\pm i\alpha} T, X_P],$$

hence (3.14) becomes

$$\begin{aligned}
X &= \frac{([i e^{\pm i\alpha} T, X_P] - \lambda \cos \alpha) ihT + h [e^{\pm i\alpha} T, X_P] T}{h} i e^{\pm i\alpha} \\
&= \{ [i e^{\pm i\alpha} T, X_P] iT - i \lambda T \cos \alpha + [e^{\pm i\alpha} T, X_P] T \} i e^{\pm i\alpha} \\
&= \left\{ -\frac{1}{2} (i e^{\pm i\alpha} T \bar{X}_P + i e^{\mp i\alpha} \bar{T} X_P) T - i \lambda T \cos \alpha + \frac{i}{2} (e^{\pm i\alpha} T \bar{X}_P - e^{\mp i\alpha} \bar{T} X_P) T \right\} i e^{\pm i\alpha} \\
&= \left\{ -\frac{i}{2} (e^{\pm i\alpha} T^2 \bar{X}_P + e^{\mp i\alpha} T \bar{T} X_P) - i \lambda T \cos \alpha + \frac{i}{2} (e^{\pm i\alpha} T^2 \bar{X}_P - e^{\mp i\alpha} T \bar{T} X_P) \right\} i e^{\pm i\alpha} \\
&= \{-i e^{\mp i\alpha} X_P - i \lambda T \cos \alpha\} i e^{\pm i\alpha} \\
&= X_P + \lambda T e^{\pm i\alpha} \cos \alpha,
\end{aligned}$$

We put $X_{F,k,\pm}(\varphi) := X$, and the proof of Theorem 3.1 is complete. \square

From Theorem 3.1 with (3.2) one easily finds the result of Corollary 3.1.

Corollary 3.1. *A parametric representation of the flank curves $X_{F,k,\pm}$ of tooth k , $k = 1, 2, \dots, z_1$, of the drive gear is given by*

$$\begin{aligned}
x_{F,k,\pm}(\varphi) &= r(\varphi) \cos \varphi - \lambda_{k,\pm}(\varphi) \cos \alpha \frac{\psi'(\varphi)(1 + \psi'(\varphi)) \sin(\varphi \mp \alpha) - \psi''(\varphi) \cos(\varphi \mp \alpha)}{w(\varphi)}, \\
y_{F,k,\pm}(\varphi) &= -r(\varphi) \sin \varphi - \lambda_{k,\pm}(\varphi) \cos \alpha \frac{\psi'(\varphi)(1 + \psi'(\varphi)) \cos(\varphi \mp \alpha) + \psi''(\varphi) \sin(\varphi \mp \alpha)}{w(\varphi)}.
\end{aligned}$$

Remark 3.1. The first Frenet formula for plane curves (see e. g. Kühnel [5, p. 10]) is

$$\frac{dT}{ds} = \kappa iT,$$

where iT is the unit normal vector which one gets by a counter-clockwise rotation of T around $\pi/2$, s the arc length, and κ the *oriented* curvature. In the case of the curve X_P we have

$$\frac{dT}{ds} = \frac{dT}{d\varphi} \frac{d\varphi}{ds} = \kappa iT \quad \Longrightarrow \quad T'(\varphi) = s'(\varphi) \kappa(\varphi) iT(\varphi). \quad (3.18)$$

Comparing (3.18) to (3.17), one sees that

$$h(\varphi) = s'(\varphi) \kappa(\varphi). \quad (3.19)$$

With

$$s'(\varphi) = \frac{d}{d\varphi} \left(a \int_{\varphi_0}^{\varphi} \frac{w(\phi)}{(1 + \psi'(\phi))^2} d\phi \right) = \frac{aw(\varphi)}{(1 + \psi'(\varphi))^2} = |X'_P(\varphi)| \quad (3.20)$$

it follows that the curvature of X_P at point φ is

$$\begin{aligned} \kappa(\varphi) &= \frac{h(\varphi)}{s'(\varphi)} = \frac{(1 + \psi'(\varphi))^2 h(\varphi)}{aw(\varphi)} \\ &= \frac{(1 + \psi'(\varphi))^3 [\psi'(\varphi) (\psi^{(3)}(\varphi) - \psi'(\varphi) - \psi'^2(\varphi)) - 2\psi''^2(\varphi)]}{aw^3(\varphi)}. \end{aligned} \quad (3.21)$$

Since it can be assumed that X_P is a regular curve, we have $s'(\varphi) = |X'_P(\varphi)| > 0$. If $\kappa(\varphi) > 0$, then $T'(\varphi)$ and $iT(\varphi)$ have equal direction, hence X_P turns to the left. If $\kappa(\varphi) < 0$, then $T'(\varphi)$ and $iT(\varphi)$ have opposite direction, hence X_P turns to the right. \triangle

The perpendicular to the flank of the rack-cutter at the currently generated point $X_{F,k,\pm}(\varphi)$ of the gear tooth flank $X_{F,k,\pm}$ passes through the instantaneous centre of velocity, $X_P(\varphi)$, of the rack-cutter motion (see [15, pp. 26-27], [7, pp. 274-275, 341-342]). Knowing this, it is possible to give a rather short alternative proof of Theorem 3.1 without using the envelope of the family of rack-cutter flank positions.

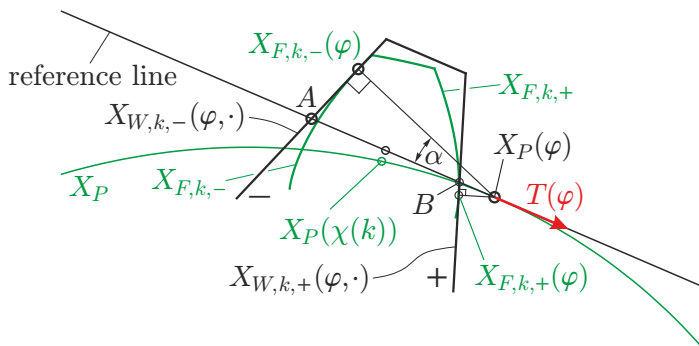


Fig. 3.3: Sketch for the short proof the Theorem 3.1

Short proof of Theorem 3.1. We consider the situation in which point $X_{F,k,-}(\varphi)$ of the flank curve $X_{F,k,-}$ is generated (see Fig. 3.3). We denote by A the intersection between the reference line and the line $X_{W,k,-}(\varphi, \cdot)$, and by μ the signed distance between A and $X_{F,k,-}(\varphi) \equiv X_{W,k,-}(\varphi, \mu)$ with $\mu > 0$ ($\mu < 0$) if $X_{F,k,-}(\varphi)$ is on the left side (right side) of the reference line with respect to the direction of vector $T(\varphi)$. The signed distance between $X_P(\varphi)$ and A is given by $\lambda_{k,-}(\varphi)$ (see (3.4) and Fig. 3.1). The points $X_P(\varphi)$, A and $X_{F,k,-}(\varphi)$ are the vertices of a rectangular triangle and thus easily follows

$$\mu = -\lambda_{k,-}(\varphi) \sin \alpha. \quad (3.22)$$

Analogously one finds the different value

$$\mu = \lambda_{k,+}(\varphi) \sin \alpha \quad (3.23)$$

for the point $X_{F,k,+}(\varphi)$ of the flank curve $X_{F,k,+}$ by considering the rectangular triangle with vertices $X_P(\varphi)$, B and $X_{F,k,+}(\varphi)$. So we can write (3.22) and (3.23) together as

$$\mu = \pm \lambda_{k,\pm}(\varphi) \sin \alpha. \quad (3.24)$$

Inserting (3.24) into (3.5), we get

$$\begin{aligned} X_{F,k,\pm}(\varphi) &= X_{W,k,\pm}(\varphi, \pm \lambda_{k,\pm}(\varphi) \sin \alpha) \\ &= X_P(\varphi) + \lambda_{k,\pm}(\varphi) (1 \pm i e^{\pm i \alpha} \sin \alpha) T(\varphi) \\ &= X_P(\varphi) + \lambda_{k,\pm}(\varphi) [1 \pm i(\cos \alpha \pm i \sin \alpha) \sin \alpha] T(\varphi) \\ &= X_P(\varphi) + \lambda_{k,\pm}(\varphi) [1 \pm (i \cos \alpha \sin \alpha \mp \sin^2 \alpha)] T(\varphi) \\ &= X_P(\varphi) + \lambda_{k,\pm}(\varphi) (1 - \sin^2 \alpha \pm i \cos \alpha \sin \alpha) T(\varphi) \\ &= X_P(\varphi) + \lambda_{k,\pm}(\varphi) (\cos^2 \alpha \pm i \cos \alpha \sin \alpha) T(\varphi) \\ &= X_P(\varphi) + \lambda_{k,\pm}(\varphi) \cos \alpha (\cos \alpha \pm i \sin \alpha) T(\varphi) \\ &= X_P(\varphi) + \lambda_{k,\pm}(\varphi) T(\varphi) e^{\pm i \alpha} \cos \alpha. \end{aligned} \quad \square$$

X_P is a negatively oriented curve. This means that an outer parallel curve is on its left side, and an inner parallel curve on its right side. Hence, with $X_P(\varphi)$ and $T(\varphi)$ according to (2.8) and (3.1), respectively, a parallel curve with distance d , $0 < d < \infty$, is given by

$$\begin{aligned} X_{p,d,\pm}(\varphi) &= X_P(\varphi) + d T(\varphi) e^{\pm i \pi / 2} = X_P(\varphi) \pm d i T(\varphi) \\ &= X_P(\varphi) \pm d i \frac{\psi''(\varphi) - i \psi'(\varphi)(1 + \psi'(\varphi))}{w(\varphi)} e^{-i \varphi} \\ &= X_P(\varphi) \pm d \frac{i \psi''(\varphi) + \psi'(\varphi)(1 + \psi'(\varphi))}{w(\varphi)} e^{-i \varphi}, \end{aligned} \quad (3.25)$$

where the upper and lower sign are for an outer and inner parallel curve, respectively; $w(\varphi)$ see (2.12). Note that our convention concerning “ \pm ” does not apply to $X_{p,d,\pm}(\varphi)$. Splitting of (3.25) into real and imaginary part yields

$$\begin{aligned} x_{p,d,\pm}(\varphi) &= r(\varphi) \cos \varphi \pm d \frac{\psi''(\varphi) \sin \varphi + \psi'(\varphi)(1 + \psi'(\varphi)) \cos \varphi}{w(\varphi)}, \\ y_{p,d,\pm}(\varphi) &= -r(\varphi) \sin \varphi \pm d \frac{\psi''(\varphi) \cos \varphi - \psi'(\varphi)(1 + \psi'(\varphi)) \sin \varphi}{w(\varphi)}. \end{aligned}$$

We denote by $X_{M,k,\pm}(\varphi)$ the parametric equation of the curve $X_{M,k,\pm}$ (see Fig. 3.2) of the mid point M_{\pm} (see Fig. 2.2). Considering Fig. 2.2, we see that

$$\tan \alpha = \frac{\ell_1}{h_f - \varrho} \quad \text{and} \quad \cos \alpha = \frac{\varrho}{\ell_2}. \quad (3.26)$$

Now, using Fig. 3.1 we find

$$\begin{aligned} X_{M,k,\pm}(\varphi) &= X_P(\varphi) + [\pm \frac{\pi m}{4} \pm \ell_1 \pm \ell_2 - a I(\chi(k), \varphi)] T(\varphi) - i(h_f - \varrho) T(\varphi) \\ &= X_P(\varphi) + [\lambda_{k,\pm}(\varphi) \pm (h_f - \varrho) \tan \alpha \pm \varrho \sec \alpha] T(\varphi) - i(h_f - \varrho) T(\varphi) \\ &= X_P(\varphi) + [\lambda_{k,\pm}(\varphi) \pm \varrho \sec \alpha - (h_f - \varrho)(i \mp \tan \alpha)] T(\varphi). \end{aligned} \quad (3.27)$$

The tangent unit vector at point $X_{M,k,\pm}(\varphi)$ of $X_{M,k,\pm}$ is given by

$$T_{M,k,\pm}(\varphi) := \frac{X'_{M,k,\pm}(\varphi)}{|X'_{M,k,\pm}(\varphi)|}.$$

From (3.27) with (3.1), (3.17) and (3.13) we obtain

$$\begin{aligned}
X'_{M,k,\pm}(\varphi) &= X'_P(\varphi) + \lambda'_{k,\pm}(\varphi) T(\varphi) + [\lambda_{k,\pm}(\varphi) \pm \varrho \sec \alpha - (h_f - \varrho)(i \mp \tan \alpha)] T'(\varphi) \\
&= \{ |X'_P(\varphi)| + \lambda'_{k,\pm}(\varphi) + [\lambda_{k,\pm}(\varphi) \pm \varrho \sec \alpha - (h_f - \varrho)(i \mp \tan \alpha)] i h(\varphi) \} T(\varphi) \\
&= [\lambda_{k,\pm}(\varphi) \pm \varrho \sec \alpha - (h_f - \varrho)(i \mp \tan \alpha)] i h(\varphi) T(\varphi).
\end{aligned}$$

The normal unit vector at point φ of the curve $X_{M,k,\pm}$ pointing to the left is given by

$$\begin{aligned}
N_{M,k,\pm}(\varphi) &= \frac{X'_{M,k,\pm}(\varphi) e^{i\pi/2}}{|X'_{M,k,\pm}(\varphi) e^{i\pi/2}|} = \frac{X'_{M,k,\pm}(\varphi) i}{|X'_{M,k,\pm}(\varphi) i|} \\
&= -\frac{[\lambda_{k,\pm}(\varphi) \pm \varrho \sec \alpha - (h_f - \varrho)(i \mp \tan \alpha)] h(\varphi) T(\varphi)}{|[\lambda_{k,\pm}(\varphi) \pm \varrho \sec \alpha - (h_f - \varrho)(i \mp \tan \alpha)] h(\varphi) T(\varphi)|} \\
&= -\frac{[\lambda_{k,\pm}(\varphi) \pm \varrho \sec \alpha - (h_f - \varrho)(i \mp \tan \alpha)] h(\varphi) T(\varphi)}{|\lambda_{k,\pm}(\varphi) \pm \varrho \sec \alpha - (h_f - \varrho)(i \mp \tan \alpha)| |h(\varphi)|} \\
&= -\operatorname{sgn}(h(\varphi)) \frac{[\lambda_{k,\pm}(\varphi) \pm \varrho \sec \alpha - (h_f - \varrho)(i \mp \tan \alpha)] T(\varphi)}{|\lambda_{k,\pm}(\varphi) \pm \varrho \sec \alpha - (h_f - \varrho)(i \mp \tan \alpha)|} \\
&= -\operatorname{sgn}(h(\varphi)) \frac{[\lambda_{k,\pm}(\varphi) \pm \varrho \sec \alpha - (h_f - \varrho)(i \mp \tan \alpha)] T(\varphi)}{\sqrt{[\lambda_{k,\pm}(\varphi) \pm \varrho \sec \alpha \pm (h_f - \varrho) \tan \alpha]^2 + (h_f - \varrho)^2}}. \tag{3.28}
\end{aligned}$$

Thus, a parametric equation of the parallel curve of interest (fillet curve), $X_{\varrho,k,\pm}$ (see Fig. 3.2), with distance ϱ to the curve $X_{M,k,\pm}$ is given by

$$X_{\varrho,k,\pm}(\varphi) = X_{M,k,\pm}(\varphi) + \varrho N_{M,k,\pm}(\varphi). \tag{3.29}$$

From (3.29) with (3.27) and (3.28) one easily gets

$$\begin{aligned}
x_{\varrho,k,\pm}(\varphi) &= r(\varphi) \cos \varphi + \left(1 - \frac{\varrho \operatorname{sgn}(h(\varphi))}{\sqrt{[\lambda_{k,\pm}(\varphi) \pm \varrho \sec \alpha \pm (h_f - \varrho) \tan \alpha]^2 + (h_f - \varrho)^2}} \right) \\
&\quad \cdot \{ [\lambda_{k,\pm}(\varphi) \pm \varrho \sec \alpha \pm (h_f - \varrho) \tan \alpha] t_x(\varphi) + (h_f - \varrho) t_y(\varphi) \}, \\
y_{\varrho,k,\pm}(\varphi) &= -r(\varphi) \sin \varphi + \left(1 - \frac{\varrho \operatorname{sgn}(h(\varphi))}{\sqrt{[\lambda_{k,\pm}(\varphi) \pm \varrho \sec \alpha \pm (h_f - \varrho) \tan \alpha]^2 + (h_f - \varrho)^2}} \right) \\
&\quad \cdot \{ [\lambda_{k,\pm}(\varphi) \pm \varrho \sec \alpha \pm (h_f - \varrho) \tan \alpha] t_y(\varphi) - (h_f - \varrho) t_x(\varphi) \}.
\end{aligned}$$

Contact point of fillet curve $X_{\varrho,k,\pm}$ and dedendum curve X_f . We determine a condition for the value of φ at the contact point of fillet curve $X_{\varrho,k,-}$ and dedendum curve $X_f := X_{p,h_f,-}$ (see Fig. 3.2; $X_{p,d,\pm}$ see (3.25)). This contact point is generated when the normal of the curve X_P at point $X_P(\varphi)$ passes through point M_- and thus also through C_- (see Fig. 3.4). In this

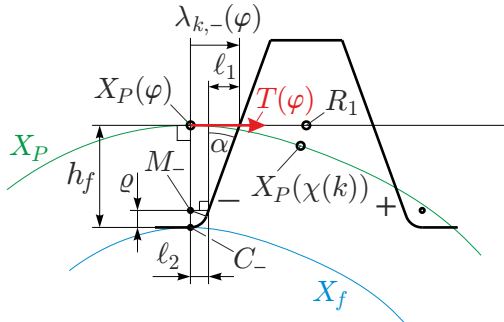


Fig. 3.4: Sketch for the situation when the contact point of $X_{\varrho,k,-}$ (not shown) and X_f is generated

situation the point C_- coincides with the contact point, and we have $\lambda_{k,-}(\varphi) = \ell_1 + \ell_2$, hence (see Fig. 2.2 and Eq. (3.26))

$$\lambda_{k,-}(\varphi) = (h_f - \varrho) \tan \alpha + \varrho \sec \alpha \quad (3.30)$$

follows as condition for the searched value of φ . Analogously, for the contact point of the fillet curve $X_{\varrho,k,+}$ and the dedendum curve X_f the formula

$$\lambda_{k,+}(\varphi) = -(h_f - \varrho) \tan \alpha - \varrho \sec \alpha \quad (3.31)$$

is obtained. We can combine (3.30) and (3.31) to

$$\mp \lambda_{k,\pm}(\varphi) = (h_f - \varrho) \tan \alpha + \varrho \sec \alpha. \quad (3.32)$$

4 Driven gear

Since both flank curves of a tooth of the drive gear are meshing with both flank curves of a tooth space of the driven gear, here we consider the flanks of the tooth spaces (see Fig. 2.3). For the generation of a tooth of the drive gear we used the flanks of a tooth space of the rack-cutter. Now, we use these flanks of the rack-cutter again, but as flanks of a tooth. This approach has the advantage that we can determine corresponding points of the flanks of the drive and the driven gear; that means: points that are in contact for a value of the drive angle φ .

From (2.7) and (2.9) we get

$$R'(\varphi) = -\frac{a\psi''(\varphi)}{(1 + \psi'(\varphi))^2} \quad \text{and} \quad \Xi'_P(\varphi) = -R'(\varphi)e^{i\psi(\varphi)} - R(\varphi)i\psi'(\varphi)e^{i\psi(\varphi)},$$

respectively, hence

$$\Xi'_P(\varphi) = \frac{a\psi''(\varphi)}{(1 + \psi'(\varphi))^2} e^{i\psi(\varphi)} - \frac{ai\psi'(\varphi)}{1 + \psi'(\varphi)} e^{i\psi(\varphi)} = \frac{a\psi''(\varphi) - ai\psi'(\varphi)(1 + \psi'(\varphi))}{(1 + \psi'(\varphi))^2} e^{i\psi(\varphi)}$$

and

$$\begin{aligned} |\Xi'_P(\varphi)| &= \left| \frac{a\psi''(\varphi)}{(1 + \psi'(\varphi))^2} - \frac{ai\psi'(\varphi)}{1 + \psi'(\varphi)} \right| \left| e^{i\psi(\varphi)} \right| = \sqrt{\frac{a^2\psi''^2(\varphi)}{(1 + \psi'(\varphi))^4} + \frac{a^2\psi'^2(\varphi)}{(1 + \psi'(\varphi))^2}} \\ &= \frac{a\sqrt{\psi''^2(\varphi) + \psi'^2(\varphi)(1 + \psi'(\varphi))^2}}{(1 + \psi'(\varphi))^2} = \frac{aw(\varphi)}{(1 + \psi'(\varphi))^2}, \end{aligned} \quad (4.1)$$

$w(\varphi)$ see (2.12). It follows that the tangent unit vector of Ξ_P at point $\Xi_P(\varphi)$ (see Fig. 4.1) is given by

$$\tilde{T}(\varphi) := \frac{\Xi'_P(\varphi)}{|\Xi'_P(\varphi)|} = \frac{\psi''(\varphi) - i\psi'(\varphi)(1 + \psi'(\varphi))}{w(\varphi)} e^{i\psi(\varphi)}. \quad (4.2)$$

Splitting (4.2) into real and imaginary part gives

$$\left. \begin{aligned} t_\xi(\varphi) &:= \operatorname{Re} \tilde{T}(\varphi) = \frac{\psi''(\varphi) \cos \psi(\varphi) + \psi'(\varphi)(1 + \psi'(\varphi)) \sin \psi(\varphi)}{w(\varphi)}, \\ t_\eta(\varphi) &:= \operatorname{Im} \tilde{T}(\varphi) = \frac{\psi''(\varphi) \sin \psi(\varphi) - \psi'(\varphi)(1 + \psi'(\varphi)) \cos \psi(\varphi)}{w(\varphi)}. \end{aligned} \right\} \quad (4.3)$$

Now we determine a parametric equation for the rack-cutter flank line $\Xi_{W,k,\pm}$ that generates flank curve $\Xi_{F,k,\pm}$ of tooth space k , $k = 1, 2, \dots, z_2$. If $\varphi = \chi(k)$, then the point R_2 of the rack-cutter coincides with the point $\Xi_P(\chi(k))$ of the centre Ξ_P (see Fig. 4.1). The vectors $\tilde{T}(\varphi)$

and $\overrightarrow{\Xi_P(\varphi)R_2}$ point into the same direction if $I(\chi(k), \varphi) < 0$. The signed arc length between the points $\Xi_P(\chi(k))$ and $\Xi_P(\varphi)$ ($=$ signed distance between R_2 and $\Xi_P(\varphi)$) is equal to $aI(\chi(k), \varphi)$. The signed distances $\lambda_{k,+}(\varphi)$ and $\lambda_{k,-}(\varphi)$ are given by (3.4). $\lambda_{k,\pm}(\varphi) > 0$ indicates that $\tilde{T}(\varphi)$ and the arrow of $\lambda_{k,\pm}(\varphi)$ have the same direction. So we have the following parametric equation for the rack-cutter flank line $\Xi_{W,k,\pm}$

$$\begin{aligned}\Xi_{W,k,\pm}(\varphi, \mu) &= \Xi_P(\varphi) + \lambda_{k,\pm}(\varphi) \tilde{T}(\varphi) + \mu \tilde{T}(\varphi) e^{i(\frac{\pi}{2} \pm \alpha)} \\ &= \Xi_P(\varphi) + \lambda_{k,\pm}(\varphi) \tilde{T}(\varphi) + \mu \tilde{T}(\varphi) ie^{\pm i\alpha} \\ &= \Xi_P(\varphi) + [\lambda_{k,\pm}(\varphi) + \mu ie^{\pm i\alpha}] \tilde{T}(\varphi), \quad \mu \in \mathbb{R}.\end{aligned}\quad (4.4)$$

Splitting of (4.4) into real and imaginary part gives

$$\left. \begin{aligned}\xi_{W,k,\pm}(\varphi, \mu) &= -R(\varphi) \cos \psi(\varphi) + \lambda_{k,\pm}(\varphi) t_\xi(\varphi) + \mu [\mp t_\xi(\varphi) \sin \alpha - t_\eta(\varphi) \cos \alpha], \\ \eta_{W,k,\pm}(\varphi, \mu) &= -R(\varphi) \sin \psi(\varphi) + \lambda_{k,\pm}(\varphi) t_\eta(\varphi) + \mu [\mp t_\eta(\varphi) \sin \alpha + t_\xi(\varphi) \cos \alpha].\end{aligned}\right\} \quad (4.5)$$

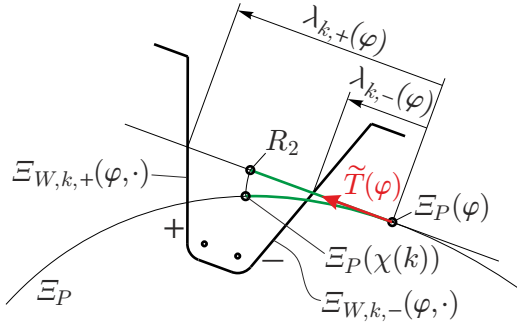


Fig. 4.1: Motion of the rack-cutter during the generation of tooth space k

Theorem 4.1. A parametric equation of the flank curves $\Xi_{F,k,\pm}$ of tooth space k , $k = 1, 2, \dots, z_2$, of the driven gear is given by

$$\Xi_{F,k,\pm}(\varphi) = \Xi_P(\varphi) + \lambda_{k,\pm}(\varphi) \tilde{T}(\varphi) e^{\pm i\alpha} \cos \alpha, \quad (4.6)$$

where

$$\begin{aligned}\Xi_P(\varphi) &= -R(\varphi) e^{i\psi(\varphi)}, \quad \tilde{T}(\varphi) = \frac{\psi''(\varphi) - i\psi'(\varphi)(1 + \psi'(\varphi))}{w(\varphi)} e^{i\psi(\varphi)}, \\ \lambda_{k,\pm}(\varphi) &= \pm \frac{\pi m}{4} - a \int_{\chi(k)}^{\varphi} \frac{w(\phi)}{(1 + \psi'(\phi))^2} d\phi\end{aligned}$$

with

$$R(\varphi) = \frac{a}{1 + \psi'(\varphi)}, \quad w(\varphi) = \sqrt{\psi''^2(\varphi) + \psi'^2(\varphi)(1 + \psi'(\varphi))^2},$$

and $\chi(k)$ according to (3.3).

Proof. The proof is completely analogous to that of Theorem 3.1. We start with the linear equation system

$$\left. \begin{aligned}[A(\varphi) - B(\varphi), \Xi] &= [A(\varphi), B(\varphi)], \\ [(A(\varphi) - B(\varphi))', \Xi] &= [A(\varphi), B(\varphi)]',\end{aligned}\right\}$$

choose

$$\begin{aligned}A &= A(\varphi) := \Xi_{W,k,\pm}(\varphi, 1) = \Xi_P(\varphi) + \lambda_{k,\pm}(\varphi) \tilde{T}(\varphi) + ie^{\pm i\alpha} \tilde{T}(\varphi), \\ B &= B(\varphi) := \Xi_{W,k,\pm}(\varphi, 0) = \Xi_P(\varphi) + \lambda_{k,\pm}(\varphi) \tilde{T}(\varphi),\end{aligned}$$

and get

$$\begin{aligned} A - B &= i e^{\pm i\alpha} \tilde{T}(\varphi), \quad (A - B)' = i e^{\pm i\alpha} \tilde{T}'(\varphi), \quad [A - B, (A - B)'] = [\tilde{T}(\varphi), \tilde{T}'(\varphi)], \\ [A, B] &= [i e^{\pm i\alpha} \tilde{T}(\varphi), \Xi_P(\varphi)] - \lambda_{k,\pm}(\varphi) \cos \alpha, \\ [A, B]' &= [i e^{\pm i\alpha} \tilde{T}'(\varphi), \Xi_P(\varphi)] - |\Xi_P'| \cos \alpha - \lambda'_{k,\pm}(\varphi) \cos \alpha. \end{aligned}$$

With

$$\lambda'_{k,\pm}(\varphi) = -|\Xi_P'(\varphi)| \quad (4.7)$$

(see (3.12) and (4.1)) we have

$$[A, B]' = [i e^{\pm i\alpha} \tilde{T}'(\varphi), \Xi_P(\varphi)].$$

It follows that (cp. (3.14))

$$\Xi = \frac{([i e^{\pm i\alpha} \tilde{T}(\varphi), \Xi_P(\varphi)] - \lambda_{k,\pm}(\varphi) \cos \alpha) \tilde{T}'(\varphi) - [i e^{\pm i\alpha} \tilde{T}'(\varphi), \Xi_P(\varphi)] \tilde{T}(\varphi)}{[\tilde{T}(\varphi), \tilde{T}'(\varphi)]} i e^{\pm i\alpha}. \quad (4.8)$$

From (4.2) one finds

$$\tilde{T}'(\varphi) = i \tilde{h}(\varphi) \tilde{T}(\varphi) \quad (4.9)$$

with the function

$$\begin{aligned} \tilde{h} : [0, 2\pi] &\rightarrow \mathbb{R} \\ \varphi &\mapsto \tilde{h}(\varphi) := \frac{(1 + \psi'(\varphi)) [\psi'(\varphi) (\psi^{(3)}(\varphi) + \psi'^2(\varphi) + \psi'^3(\varphi)) - \psi''^2(\varphi)]}{w^2(\varphi)}. \end{aligned} \quad (4.10)$$

Plugging (4.9) into (4.8) finally gives

$$\Xi = \Xi_P(\varphi) + \lambda_{k,\pm}(\varphi) \tilde{T}(\varphi) e^{\pm i\alpha} \cos \alpha.$$

We put $\Xi_{F,k,\pm}(\varphi) := \Xi$ which completes the proof of Theorem 4.1. \square

From Theorem 4.1 with (4.3) one concludes the result of Corollary 4.1.

Corollary 4.1. *A parametric representation of the flank curves $\Xi_{F,k,\pm}$ of tooth space k , $k = 1, 2, \dots, z_2$, of the driven gear is given by*

$$\begin{aligned} \xi_{F,k,\pm}(\varphi) &= -R(\varphi) \cos \psi(\varphi) \\ &\quad + \lambda_{k,\pm}(\varphi) \cos \alpha \frac{\psi''(\varphi) \cos(\psi(\varphi) \pm \alpha) + \psi'(\varphi)(1 + \psi'(\varphi)) \sin(\psi(\varphi) \pm \alpha)}{w(\varphi)}, \\ \eta_{F,k,\pm}(\varphi) &= -R(\varphi) \sin \psi(\varphi) \\ &\quad + \lambda_{k,\pm}(\varphi) \cos \alpha \frac{\psi''(\varphi) \sin(\psi(\varphi) \pm \alpha) - \psi'(\varphi)(1 + \psi'(\varphi)) \cos(\psi(\varphi) \pm \alpha)}{w(\varphi)}. \end{aligned}$$

Remark 4.1. The first Frenet formula in the case of the curve Ξ_P is

$$\frac{d\tilde{T}}{ds} = \tilde{\kappa} i \tilde{T},$$

where s is the arc length and $\tilde{\kappa}$ the oriented curvature. We have

$$\frac{d\tilde{T}}{ds} = \frac{d\tilde{T}}{d\varphi} \frac{d\varphi}{ds} = \kappa i \tilde{T} \implies \tilde{T}'(\varphi) = s'(\varphi) \tilde{\kappa}(\varphi) i \tilde{T}(\varphi). \quad (4.11)$$

Comparing (4.11) to (4.9), one sees that

$$\tilde{h}(\varphi) = s'(\varphi) \tilde{\kappa}(\varphi). \quad (4.12)$$

With

$$s'(\varphi) = |\Xi'_P(\varphi)| \quad (4.13)$$

(see (3.20) and (4.1)), it follows that the curvature of Ξ_P at point φ is

$$\begin{aligned} \tilde{\kappa}(\varphi) &= \frac{\tilde{h}(\varphi)}{s'(\varphi)} = \frac{(1 + \psi'(\varphi))^2 \tilde{h}(\varphi)}{aw(\varphi)} \\ &= \frac{(1 + \psi'(\varphi))^3 [\psi^{(3)}(\varphi) + \psi'^2(\varphi) + \psi'^3(\varphi)] - \psi''^2(\varphi)}{aw^3(\varphi)}. \end{aligned} \quad (4.14)$$

Since it can be assumed that Ξ_P is a regular curve, we have $s'(\varphi) = |\Xi'_P(\varphi)| > 0$. If $\tilde{\kappa}(\varphi) > 0$, then $\tilde{T}'(\varphi)$ and $i\tilde{T}(\varphi)$ have equal direction, hence Ξ_P turns to the left. If $\tilde{\kappa}(\varphi) < 0$, then $\tilde{T}'(\varphi)$ and $i\tilde{T}(\varphi)$ have opposite direction, hence Ξ_P turns to the right. \triangle

As for Theorem 3.1, we give a short proof of Theorem 4.1 which uses the fact that the perpendicular to the flank of the rack-cutter at the currently generated point of the gear tooth flank passes through the instantaneous centre of velocity of the motion of the rack-cutter.

Short proof of Theorem 4.1. The value of the parameter μ at the contact point $\Xi_{W,k,\pm}(\varphi, \mu) \equiv \Xi_{F,k,\pm}(\varphi)$ between rack-cutter flank line $\Xi_{W,k,\pm}(\varphi, \cdot)$ and tooth flank curve $\Xi_{F,k,\pm}$ to be generated is given by (3.24). Therefore, applying (4.4), we get

$$\begin{aligned} \Xi_{F,k,\pm}(\varphi) &= \Xi_{W,k,\pm}(\varphi, \pm \lambda_{k,\pm}(\varphi) \sin \alpha) \\ &= \Xi_P(\varphi) + \lambda_{k,\pm}(\varphi) (1 \pm i e^{\pm i \alpha} \sin \alpha) \tilde{T}(\varphi) \\ &= \Xi_P(\varphi) + \lambda_{k,\pm}(\varphi) \tilde{T}(\varphi) e^{\pm i \alpha} \cos \alpha. \end{aligned} \quad \square$$

Ξ_P is a positively oriented curve. An outer parallel curve is on its right side, and an inner parallel curve on its left side. Therefore, with $\Xi_P(\varphi)$ and $\tilde{T}(\varphi)$ according to (2.9) and (4.2), respectively, a parallel curve with distance d , $0 < d < \infty$, is given by

$$\begin{aligned} \Xi_{p,d,\pm}(\varphi) &= \Xi_P(\varphi) + d \tilde{T}(\varphi) e^{\mp i \pi/2} = \Xi_P(\varphi) \mp d i \tilde{T}(\varphi) \\ &= \Xi_P(\varphi) \mp d i \frac{\psi''(\varphi) - i \psi'(\varphi)(1 + \psi'(\varphi))}{w(\varphi)} e^{i \psi(\varphi)} \\ &= \Xi_P(\varphi) \mp d \frac{\psi'(\varphi)(1 + \psi'(\varphi)) + i \psi''(\varphi)}{w(\varphi)} e^{i \psi(\varphi)}, \end{aligned} \quad (4.15)$$

where the upper and lower sign are for the outer and inner parallel curve, respectively; $w(\varphi)$ see (2.12). Note that our convention concerning “ \pm ” does not apply to $\Xi_{p,d,\pm}(\varphi)$. Splitting of (4.15) into real and imaginary part yields

$$\begin{aligned} \xi_{p,d,\pm}(\varphi) &= -R(\varphi) \cos \psi(\varphi) \mp d \frac{\psi'(\varphi)(1 + \psi'(\varphi)) \cos \psi(\varphi) - \psi''(\varphi) \sin \psi(\varphi)}{w(\varphi)}, \\ \eta_{p,d,\pm}(\varphi) &= -R(\varphi) \sin \psi(\varphi) \mp d \frac{\psi'(\varphi)(1 + \psi'(\varphi)) \sin \psi(\varphi) + \psi''(\varphi) \cos \psi(\varphi)}{w(\varphi)}. \end{aligned}$$

We denote by $\Xi_{M,k,\pm}(\varphi)$ the parametric equation of the curve $\Xi_{M,k,\pm}$ of the mid point M_{\pm} in Fig. 2.2 where M_- is the right one. We have

$$\begin{aligned}\Xi_{M,k,\pm}(\varphi) &= \Xi_P(\varphi) + \left[\pm \frac{\pi m}{4} \mp (h_f - \varrho) \tan \alpha \mp \varrho \sec \alpha - aI(\chi(k), \varphi) \right] \tilde{T}(\varphi) \\ &\quad + i(h_f - \varrho) \tilde{T}(\varphi) \\ &= \Xi_P(\varphi) + [\lambda_{k,\pm}(\varphi) \mp \varrho \sec \alpha + (h_f - \varrho)(i \mp \tan \alpha)] \tilde{T}(\varphi).\end{aligned}\quad (4.16)$$

The tangent unit vector at point $\Xi_{M,k,\pm}(\varphi)$ of $\Xi_{M,k,\pm}$ is given by

$$\tilde{T}_{M,k,\pm}(\varphi) := \frac{\Xi'_{M,k,\pm}(\varphi)}{|\Xi'_{M,k,\pm}(\varphi)|}.$$

From (4.16) with (4.2), (4.9) and (4.7) we obtain

$$\begin{aligned}\Xi'_{M,k,\pm}(\varphi) &= \Xi'_P(\varphi) + \lambda'_{k,\pm}(\varphi) \tilde{T}(\varphi) + [\lambda_{k,\pm}(\varphi) \mp \varrho \sec \alpha + (h_f - \varrho)(i \mp \tan \alpha)] \tilde{T}'(\varphi) \\ &= \{ |\Xi'_P(\varphi)| + \lambda'_{k,\pm}(\varphi) + [\lambda_{k,\pm}(\varphi) \mp \varrho \sec \alpha + (h_f - \varrho)(i \mp \tan \alpha)] i \tilde{h}(\varphi) \} \tilde{T}(\varphi) \\ &= [\lambda_{k,\pm}(\varphi) \mp \varrho \sec \alpha + (h_f - \varrho)(i \mp \tan \alpha)] i \tilde{h}(\varphi) \tilde{T}(\varphi).\end{aligned}$$

The normal unit vector at point φ of the curve $\Xi_{M,k,\pm}$ pointing to the right is given by

$$\begin{aligned}\tilde{N}_{M,k,\pm}(\varphi) &= \frac{\Xi'_{M,k,\pm}(\varphi) e^{-i\pi/2}}{|\Xi'_{M,k,\pm}(\varphi) e^{-i\pi/2}|} = -\frac{\Xi'_{M,k,\pm}(\varphi) i}{|\Xi'_{M,k,\pm}(\varphi) i|} \\ &= \frac{[\lambda_{k,\pm}(\varphi) \mp \varrho \sec \alpha + (h_f - \varrho)(i \mp \tan \alpha)] \tilde{h}(\varphi) \tilde{T}(\varphi)}{|[\lambda_{k,\pm}(\varphi) \mp \varrho \sec \alpha + (h_f - \varrho)(i \mp \tan \alpha)] \tilde{h}(\varphi) \tilde{T}(\varphi)|} \\ &= \frac{[\lambda_{k,\pm}(\varphi) \mp \varrho \sec \alpha + (h_f - \varrho)(i \mp \tan \alpha)] \tilde{h}(\varphi) \tilde{T}(\varphi)}{|\lambda_{k,\pm}(\varphi) \mp \varrho \sec \alpha + (h_f - \varrho)(i \mp \tan \alpha)| |\tilde{h}(\varphi)|} \\ &= \operatorname{sgn}(\tilde{h}(\varphi)) \frac{[\lambda_{k,\pm}(\varphi) \mp \varrho \sec \alpha + (h_f - \varrho)(i \mp \tan \alpha)] \tilde{T}(\varphi)}{|\lambda_{k,\pm}(\varphi) \mp \varrho \sec \alpha + (h_f - \varrho)(i \mp \tan \alpha)|} \\ &= \operatorname{sgn}(\tilde{h}(\varphi)) \frac{[\lambda_{k,\pm}(\varphi) \mp \varrho \sec \alpha + (h_f - \varrho)(i \mp \tan \alpha)] \tilde{T}(\varphi)}{\sqrt{[\lambda_{k,\pm}(\varphi) \mp \varrho \sec \alpha \mp (h_f - \varrho) \tan \alpha]^2 + (h_f - \varrho)^2}}.\end{aligned}\quad (4.17)$$

Thus,

$$\Xi_{\varrho,k,\pm}(\varphi) = \Xi_{M,k,\pm}(\varphi) + \varrho \tilde{N}_{M,k,\pm}(\varphi) \quad (4.18)$$

is a parametric equation of the parallel curve of interest (fillet curve), $\Xi_{\varrho,k,\pm}$, with distance ϱ to curve $\Xi_{M,k,\pm}$. From (4.18) with (4.16) and (4.17) one easily gets

$$\begin{aligned}\xi_{\varrho,k,\pm}(\varphi) &= -R(\varphi) \cos \psi(\varphi) + \left(1 + \frac{\varrho \operatorname{sgn}(\tilde{h}(\varphi))}{\sqrt{[\lambda_{k,\pm}(\varphi) \mp \varrho \sec \alpha \mp (h_f - \varrho) \tan \alpha]^2 + (h_f - \varrho)^2}} \right) \\ &\quad \cdot \{ [\lambda_{k,\pm}(\varphi) \mp \varrho \sec \alpha \mp (h_f - \varrho) \tan \alpha] t_{\xi}(\varphi) - (h_f - \varrho) t_{\eta}(\varphi) \}, \\ \eta_{\varrho,k,\pm}(\varphi) &= -R(\varphi) \sin \psi(\varphi) + \left(1 + \frac{\varrho \operatorname{sgn}(\tilde{h}(\varphi))}{\sqrt{[\lambda_{k,\pm}(\varphi) \mp \varrho \sec \alpha \mp (h_f - \varrho) \tan \alpha]^2 + (h_f - \varrho)^2}} \right) \\ &\quad \cdot \{ [\lambda_{k,\pm}(\varphi) \mp \varrho \sec \alpha \mp (h_f - \varrho) \tan \alpha] t_{\eta}(\varphi) + (h_f - \varrho) t_{\xi}(\varphi) \}.\end{aligned}$$

Contact point of fillet curve $\Xi_{\varrho,k,\pm}$ and dedendum curve Ξ_f . One finds

$$\pm \lambda_{k,\pm}(\varphi) = (h_f - \varrho) \tan \alpha + \varrho \sec \alpha \quad (4.19)$$

as condition for the value of φ at the contact point of $\Xi_{\varrho,k,\pm}$ and $\Xi_f := \Xi_{p,h_f,-}$ ($\Xi_{p,d,\pm}$ see (4.15)).

5 Undercut

5.1 Drive gear (undercut)

There are two cases for the transition between the fillet curve $X_{\varrho,k,\pm}$ and the working part of the flank curve $X_{F,k,\pm}$:

- $X_{\varrho,k,\pm}$ and the working part of $X_{F,k,\pm}$ have a common tangent direction at the *transition point*. It is said that the flank is free of *undercut*.
- $X_{\varrho,k,\pm}$ and the working part $X_{F,k,\pm}$ have no common tangent direction at the *transition point*. It is said that *undercut* occurs at the flank.

Normally, there exists always exactly one *contact point* of $X_{\varrho,k,\pm}$ and $X_{F,k,\pm}$ where both curves have a common tangent direction. In case (a) the transition point is the contact point, in case (b) not.

We consider the “-”-side of the gear tooth. Undercut occurs if the value $\varphi_{B,k,-}$ of the parameter φ at the contact point of $X_{F,k,-}$ and $X_{\varrho,k,-}$ is smaller than then value $\varphi_{S,k,-}$ of φ at the singular point (cusp) of $X_{F,k,-}$. On the “+”-side we have the reverse situation: Undercut occurs if the value $\varphi_{B,k,+}$ of φ at the contact point of $X_{F,k,+}$ and $X_{\varrho,k,+}$ is greater than the value $\varphi_{S,k,+}$ of φ at the singular point (cusp) of $X_{F,k,+}$. One gets the values $\varphi_{S,k,\pm}$ by deriving $X_{F,k,\pm}(\varphi)$ (see (3.7)) with respect to φ , and then setting the result equal to zero,

$$X'_{F,k,\pm}(\varphi_{S,k,\pm}) = \frac{dX_{F,k,\pm}}{d\varphi}(\varphi_{S,\pm}) = 0. \quad (5.1)$$

Applying (3.1), (3.13) and (3.17), we have

$$\begin{aligned} X'_{F,k,\pm}(\varphi) &= X'_P(\varphi) + (\lambda'_{k,\pm}(\varphi) T(\varphi) + \lambda_{k,\pm}(\varphi) T'(\varphi)) e^{\pm i\alpha} \cos \alpha \\ &= |X'_P(\varphi)| T(\varphi) + (\lambda'_{k,\pm}(\varphi) + \lambda_{k,\pm}(\varphi) ih(\varphi)) T(\varphi) e^{\pm i\alpha} \cos \alpha \\ &= [-\lambda'_{k,\pm}(\varphi) + (\lambda'_{k,\pm}(\varphi) + \lambda_{k,\pm}(\varphi) ih(\varphi)) (\cos \alpha \pm i \sin \alpha) \cos \alpha] T(\varphi) \\ &= [-\lambda'_{k,\pm}(\varphi) + \lambda'_{k,\pm}(\varphi) (\cos^2 \alpha \pm i \sin \alpha \cos \alpha) \\ &\quad + \lambda_{k,\pm}(\varphi) h(\varphi) (i \cos^2 \alpha \mp \sin \alpha \cos \alpha)] T(\varphi) \\ &= [-\lambda'_{k,\pm}(\varphi) + \lambda'_{k,\pm}(\varphi) \cos^2 \alpha \mp \lambda_{k,\pm}(\varphi) h(\varphi) \sin \alpha \cos \alpha \\ &\quad + i (\lambda_{k,\pm}(\varphi) h(\varphi) \cos^2 \alpha \pm \lambda'_{k,\pm}(\varphi) \sin \alpha \cos \alpha)] T(\varphi) \\ &= [-\lambda'_{k,\pm}(\varphi) \sin^2 \alpha \mp \lambda_{k,\pm}(\varphi) h(\varphi) \sin \alpha \cos \alpha \\ &\quad + i (\lambda_{k,\pm}(\varphi) h(\varphi) \cos^2 \alpha \pm \lambda'_{k,\pm}(\varphi) \sin \alpha \cos \alpha)] T(\varphi) \\ &= [-(\lambda'_{k,\pm}(\varphi) \sin \alpha \pm \lambda_{k,\pm}(\varphi) h(\varphi) \cos \alpha) \sin \alpha \\ &\quad + i (\lambda_{k,\pm}(\varphi) h(\varphi) \cos \alpha \pm \lambda'_{k,\pm}(\varphi) \sin \alpha) \cos \alpha] T(\varphi). \end{aligned}$$

From the condition (5.1) it follows that the term in the square brackets is equal to zero, and so real and imaginary part of this term are equal to zero which gives

$$\lambda_{k,\pm}(\varphi) h(\varphi) \cos \alpha \pm \lambda'_{k,\pm}(\varphi) \sin \alpha = 0,$$

hence

$$\lambda_{k,\pm}(\varphi) h(\varphi) = \mp \lambda'_{k,\pm}(\varphi) \tan \alpha.$$

Using (3.19) and $s'(\varphi) = -\lambda'_{k,\pm}(\varphi)$ (cp. (3.12) and (3.20)), we get

$$-\lambda_{k,\pm}(\varphi) \lambda'_{k,\pm}(\varphi) \kappa(\varphi) = \mp \lambda'_{k,\pm}(\varphi) \tan \alpha.$$

So, we have

$$\lambda_{k,\pm}(\varphi) \kappa(\varphi) = \pm \tan \alpha \quad (5.2)$$

as condition for the value $\varphi_{S,k,\pm}$ of φ at the singular point of $X_{F,k,\pm}$.

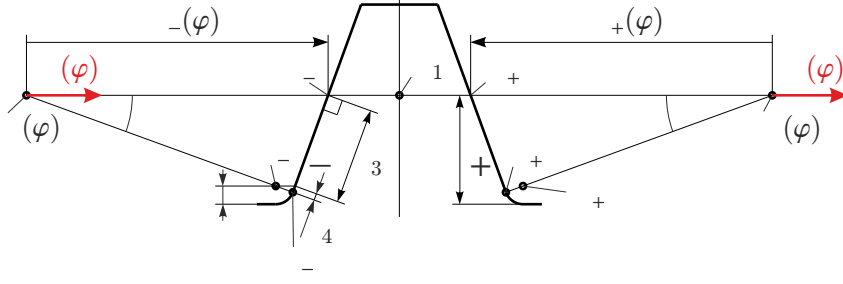


Fig. 5.1: Sketch for the situation when the contact point of $X_{F,k,\pm}$ and $X_{\varrho,k,\pm}$ is generated

Now, we determine a condition for the value of φ at the contact point of $X_{F,k,\pm}$ and $X_{\varrho,k,\pm}$ (see Fig. 3.2). We denote by D_{\pm} the point where the rack-cutter “ \pm ”-flank is tangent to its rack-cutter fillet (see Fig. 5.1). When the contact point is generated, the rack-cutter “ \pm ”-flank at its point D_{\pm} is tangent to $X_{F,k,\pm}$ (not shown), and at the same time to $X_{\varrho,k,\pm}$ (also not shown). So the rectangular triangle $D_{\pm}E_{\pm}X_P(\varphi)$ gives

$$\sin \alpha = \frac{\ell_3 + \ell_4}{\mp \lambda_{k,\pm}(\varphi)},$$

where, for ℓ_4 see also Fig. 2.2,

$$\ell_3 = (h_f - \varrho) \sec \alpha, \quad \ell_4 = \varrho \tan \alpha,$$

hence

$$\mp \lambda_{k,\pm}(\varphi) = \frac{h_f - \varrho}{\cos \alpha \sin \alpha} + \frac{\varrho}{\cos \alpha},$$

and therefore

$$\mp \lambda_{k,\pm}(\varphi) \cos \alpha = (h_f - \varrho) \csc \alpha + \varrho. \quad (5.3)$$

This is the condition for the value $\varphi_{B,k,\pm}$ of the parameter φ at the contact point. We write the condition (5.2) for the singular point as

$$\lambda_{k,\pm}(\varphi) \cos \alpha = \pm \frac{\sin \alpha}{\kappa(\varphi)}. \quad (5.4)$$

Since the functions $\lambda_{k,\pm}(\varphi)$ are strictly decreasing, and the non-undercutting conditions are

$$\varphi_{S,k,-} \leq \varphi_{B,k,-} \quad \text{and} \quad \varphi_{S,k,+} \geq \varphi_{B,k,+},$$

we have

$$\lambda_{k,-}(\varphi_{S,k,-}) \geq \lambda_{k,-}(\varphi_{B,k,-}) \quad \text{and} \quad \lambda_{k,+}(\varphi_{S,k,+}) \leq \lambda_{k,+}(\varphi_{B,k,+}).$$

Therefore, from (5.3), (5.4), and $\cos \alpha > 0$, $0 \leq \alpha < \pi/2$, one gets

$$-\frac{\sin \alpha}{\kappa(\varphi_{S,k,-})} \geq (h_f - \varrho) \csc \alpha + \varrho \quad \text{and} \quad \frac{\sin \alpha}{\kappa(\varphi_{S,k,+})} \leq -(h_f - \varrho) \csc \alpha - \varrho.$$

Putting together these inequalities, we have

$$\frac{\sin \alpha}{-\kappa(\varphi_{S,k,\pm})} \geq (h_f - \varrho) \csc \alpha + \varrho.$$

Since $\kappa(\varphi) \leq 0$, $0 \leq \varphi \leq 2\pi$, we have $-\kappa(\varphi_{S,k,\pm}) \geq 0$ and

$$-\kappa(\varphi_{S,k,\pm}) \leq \frac{\sin \alpha}{(h_f - \varrho) \csc \alpha + \varrho} = \frac{\sin^2 \alpha}{h_f - \varrho + \varrho \sin \alpha}.$$

So we have found the following theorem.

Theorem 5.1. *The “ \pm ”-flank of tooth k , $k = 1, 2, \dots, z_1$, of the drive gear is free of undercut if*

$$-\kappa(\varphi_{S,k,\pm}) \leq \frac{\sin^2 \alpha}{h_f - \varrho(1 - \sin \alpha)}, \quad (5.5)$$

where

- $\kappa(\varphi)$ is the curvature at point $X_P(\varphi)$ of the centrod X_P according to (3.21),
- $\varphi_{S,k,\pm}$ the value of φ at the singular point (cusp) of $X_{F,k,\pm}$ which is the solution of (5.2),
- α , h_f and ϱ are the profile angle, the dedendum and the fillet radius, respectively (see Fig. 2.2).

Note that, besides α , h_f and ϱ , the condition (5.5) depends only on the curvature $\kappa(\varphi)$ of the centrod X_P at the only point $X_P(\varphi_{S,k,\pm})$. So, in order to check if tooth k is free of undercut, it is necessary to determine the singular points $\varphi_{S,k,\pm}$ from (5.2) and then use (5.5).

Corollary 5.1. *Every tooth of the drive gear is free of undercut if*

$$-\kappa(\varphi) \leq \frac{\sin^2 \alpha}{h_f - \varrho(1 - \sin \alpha)} \quad \text{for } 0 \leq \varphi \leq 2\pi. \quad (5.6)$$

Introducing the dimensionless quantities

$$h_f^* := \frac{h_f}{m} \quad \text{and} \quad \varrho^* := \frac{\varrho}{m}, \quad (5.7)$$

from (5.6) we get the condition

$$m \leq \frac{\sin^2 \alpha}{(h_f^* - \varrho^*(1 - \sin \alpha)) \max_{0 \leq \varphi \leq 2\pi} (-\kappa(\varphi))} \quad (5.8)$$

for the values of the module m which provide that every tooth of the drive gear is free of undercut. h_f^* and ϱ^* in (5.8) can be freely chosen within reasonable limits, e.g. according to the rack-cutters available or to DIN 3972 [3]. Note that $\kappa(\varphi)$ depends on the pivot distance $a = \overline{O_1 O_2}$. A greater value of a yields a smaller value of $\max_{0 \leq \varphi \leq 2\pi} (-\kappa(\varphi))$; hence greater values of m are possible. On the other hand, the chosen value of m influences a . From (5.8) with (3.21) one gets

$$\frac{m}{a} \leq \frac{\sin^2 \alpha}{(h_f^* - \varrho^*(1 - \sin \alpha)) \max_{0 \leq \varphi \leq 2\pi} \left| \frac{(1 + \psi'(\varphi))^2 h(\varphi)}{w(\varphi)} \right|},$$

hence

$$\frac{a}{m} \geq \frac{h_f^* - \varrho^*(1 - \sin \alpha)}{\sin^2 \alpha} \max_{0 \leq \varphi \leq 2\pi} \left| \frac{(1 + \psi'(\varphi))^2 h(\varphi)}{w(\varphi)} \right|. \quad (5.9)$$

Inequality (5.9) provides an useful criterion to determine pivot distance a and module m if undercut is not allowed. The ratio a/m can be considered as *dimensionless pivot distance* in a certain sense. (Clearly, for $m = 1$ mm it is the real pivot distance without the unit “mm”.) With (2.14) we get

$$z_1 \geq \frac{I(0, 2\pi) (h_f^* - \varrho^*(1 - \sin \alpha))}{\pi \sin^2 \alpha} \max_{0 \leq \varphi \leq 2\pi} \left| \frac{(1 + \psi'(\varphi))^2 h(\varphi)}{w(\varphi)} \right|$$

as criterion for the number z_1 of teeth necessary to ensure that each tooth is free of undercut.

5.2 Driven gear (undercut)

We determine the singular point $\tilde{\varphi}_{S,k,\pm}$ of $\Xi_{F,k,\pm}$. It follows from the condition

$$\Xi'_{F,k,\pm}(\tilde{\varphi}_{S,k,\pm}) = 0. \quad (5.10)$$

Applying (4.2), (4.9) and (4.7), we have

$$\begin{aligned} \Xi'_{F,k,\pm}(\varphi) &= \Xi'_P(\varphi) + \left(\lambda'_{k,\pm}(\varphi) \tilde{T}(\varphi) + \lambda_{k,\pm}(\varphi) \tilde{T}'(\varphi) \right) e^{\pm i\alpha} \cos \alpha \\ &= |\Xi'_P(\varphi)| \tilde{T}(\varphi) + \left(-|\Xi'_P(\varphi)| + \lambda_{k,\pm}(\varphi) i \tilde{h}(\varphi) \right) \tilde{T}(\varphi) e^{\pm i\alpha} \cos \alpha \\ &= \left[|\Xi'_P(\varphi)| + \left(-|\Xi'_P(\varphi)| + \lambda_{k,\pm}(\varphi) i \tilde{h}(\varphi) \right) (\cos \alpha \pm i \sin \alpha) \cos \alpha \right] \tilde{T}(\varphi) \\ &= \left[\left(|\Xi'_P(\varphi)| \sin \alpha \mp \lambda_{k,\pm}(\varphi) \tilde{h}(\varphi) \cos \alpha \right) \sin \alpha \right. \\ &\quad \left. + i \left(\lambda_{k,\pm}(\varphi) \tilde{h}(\varphi) \cos \alpha \mp |\Xi'_P(\varphi)| \sin \alpha \right) \cos \alpha \right] \tilde{T}(\varphi). \end{aligned}$$

From (5.10) it follows that the term in the square brackets is equal to zero, and so real and imaginary part of this term are equal to zero which gives

$$\lambda_{k,\pm}(\varphi) \tilde{h}(\varphi) \cos \alpha \mp |\Xi'_P(\varphi)| \sin \alpha = 0,$$

hence

$$\lambda_{k,\pm}(\varphi) \tilde{h}(\varphi) = \pm |\Xi'_P(\varphi)| \tan \alpha.$$

Using (4.12) and (4.13), we get

$$\lambda_{k,\pm}(\varphi) \tilde{\kappa}(\varphi) = \pm \tan \alpha \quad (5.11)$$

as condition for the values $\tilde{\varphi}_{S,k,\pm}$ of φ at the singular points of $\Xi_{F,k,\pm}$. One finds

$$\pm \lambda_{k,\pm}(\varphi) \cos \alpha = (h_f - \varrho) \csc \alpha + \varrho \quad (5.12)$$

as condition for the value $\tilde{\varphi}_{B,k,\pm}$ of φ at the contact point of $\Xi_{F,k,\pm}$ and $\Xi_{\varrho,k,\pm}$. Finally, one gets the following theorem.

Theorem 5.2. *The “ \pm ”-flank of tooth space k , $k = 1, 2, \dots, z_2$, of the driven gear is free of undercut if*

$$\tilde{\kappa}(\tilde{\varphi}_{S,k,\pm}) \leq \frac{\sin^2 \alpha}{h_f - \varrho(1 - \sin \alpha)}, \quad (5.13)$$

where

- $\tilde{\kappa}(\varphi)$ is the curvature at point $\Xi_P(\varphi)$ of the centrod Ξ_P according to (4.14),
- $\tilde{\varphi}_{S,k,\pm}$ the value of φ at the singular point (cusp) of $\Xi_{F,k,\pm}$ which is the solution of (5.11),
- α , h_f and ϱ are the profile angle, the dedendum and the fillet radius, respectively (see Fig. 2.2).

Corollary 5.2. *Every tooth of the driven gear is free of undercut if*

$$\tilde{\kappa}(\varphi) \leq \frac{\sin^2 \alpha}{h_f - \varrho(1 - \sin \alpha)} \quad \text{for } 0 \leq \varphi \leq 2\pi. \quad (5.14)$$

6 The base curves

Unidirectional flanks of different teeth of a gear, i.e. all “+”-flanks or all “-”-flanks, can be generated as involutes of a so-called *base curve* [15, p. 241]. The respective base curve is the evolute of all unidirectional flanks.

6.1 Base curve of the drive gear

The following theorem establishes a parametric equation for the base curves $X_{B,\pm}$ of the drive gear.

Lemma 6.1. *A parametric equation of the base curves $X_{B,\pm}$ of the drive gear is given by*

$$X_{B,\pm}(\varphi) = X_P(\varphi) \pm \frac{\sin \alpha}{\kappa(\varphi)} T(\varphi) e^{\pm i\alpha}, \quad 0 \leq \varphi \leq 2\pi, \quad (6.1)$$

where $\kappa(\varphi)$ and $T(\varphi)$ are the curvature and the tangent unit vector, respectively, of the centrode X_P at point φ .

Proof. The base curve is obtained as the envelope of all straight lines that intersect the centrode at the same angle α [15, p. 241]. The two straight lines that intersect the centrode X_P at point φ with the angles $-\alpha$ and $+\alpha$, respectively, are given by

$$X = X_P(\varphi) + \mu T(\varphi) e^{\pm i\alpha}, \quad \mu \in \mathbb{R}. \quad (6.2)$$

Now we use (3.10), and choose, with $\mu = 1$ and $\mu = 0$, respectively, in (6.2),

$$\begin{aligned} A &= A(\varphi) := X_P(\varphi) + T(\varphi) e^{\pm i\alpha}, \\ B &= B(\varphi) := X_P(\varphi). \end{aligned}$$

We have

$$A(\varphi) - B(\varphi) = T(\varphi) e^{\pm i\alpha}$$

and, see (3.17),

$$(A(\varphi) - B(\varphi))' = T'(\varphi) e^{\pm i\alpha} = i h(\varphi) T(\varphi) e^{\pm i\alpha}.$$

With this one finds

$$\begin{aligned} [A - B, (A - B)'] &= [T e^{\pm i\alpha}, i h T e^{\pm i\alpha}] = h [T e^{\pm i\alpha}, i T e^{\pm i\alpha}] = h T e^{\pm i\alpha} \overline{T e^{\pm i\alpha}} [1, i] \\ &= h T \bar{T} e^{\pm i\alpha} e^{\mp i\alpha} [1, i] = h. \end{aligned}$$

One also gets

$$[A, B] = [X_P + T e^{\pm i\alpha}, X_P] = [X_P, X_P] + [T e^{\pm i\alpha}, X_P] = [T e^{\pm i\alpha}, X_P]$$

and

$$\begin{aligned} [A, B]' &= [T e^{\pm i\alpha}, X_P]' = [T' e^{\pm i\alpha}, X_P] + [T e^{\pm i\alpha}, X_P'] = [i h T e^{\pm i\alpha}, X_P] + [T e^{\pm i\alpha}, |X_P'| T] \\ &= h [i T e^{\pm i\alpha}, X_P] + |X_P'| [T e^{\pm i\alpha}, T] = h [i T e^{\pm i\alpha}, X_P] + |X_P'| T \bar{T} [e^{\pm i\alpha}, 1] \\ &= h [i T e^{\pm i\alpha}, X_P] - |X_P'| [1, e^{\pm i\alpha}] = h [i T e^{\pm i\alpha}, X_P] - |X_P'| \operatorname{Im} e^{\pm i\alpha} \\ &= h [i T e^{\pm i\alpha}, X_P] \mp |X_P'| \sin \alpha. \end{aligned}$$

Thus we obtain by means of (3.10)

$$\begin{aligned} X &= \frac{[T e^{\pm i\alpha}, X_P] i h T e^{\pm i\alpha} - (h [i T e^{\pm i\alpha}, X_P] \mp |X_P'| \sin \alpha) T e^{\pm i\alpha}}{h} \\ &= \frac{([T e^{\pm i\alpha}, X_P] i - [i T e^{\pm i\alpha}, X_P]) h \pm |X_P'| \sin \alpha}{h} T e^{\pm i\alpha} \\ &= ([T e^{\pm i\alpha}, X_P] i - [i T e^{\pm i\alpha}, X_P]) T e^{\pm i\alpha} \pm \frac{1}{h} |X_P'| T e^{\pm i\alpha} \sin \alpha. \end{aligned}$$

Now we get

$$\begin{aligned}
& T e^{\pm i\alpha}, X_P] i - [i T e^{\pm i\alpha}, X_P] \\
&= -\frac{1}{2} (T e^{\pm i\alpha} \bar{X}_P - \bar{T} e^{\mp i\alpha} X_P) - \frac{i}{2} (i T e^{\pm i\alpha} \bar{X}_P + i \bar{T} e^{\mp i\alpha} X_P) \\
&= -\frac{1}{2} (T e^{\pm i\alpha} \bar{X}_P - \bar{T} e^{\mp i\alpha} X_P) + \frac{1}{2} (T e^{\pm i\alpha} \bar{X}_P + \bar{T} e^{\mp i\alpha} X_P) \\
&= \bar{T} e^{\mp i\alpha} X_P,
\end{aligned}$$

hence

$$X = X_P \pm \frac{1}{h} |X'_P| T e^{\pm i\alpha} \sin \alpha.$$

With (3.20) and (3.21) we have

$$|X'_P(\varphi)| = \frac{h(\varphi)}{\kappa(\varphi)}, \quad (6.3)$$

and so finally follows

$$X = X_P(\varphi) \pm \frac{\sin \alpha}{\kappa(\varphi)} T(\varphi) e^{\pm i\alpha}. \quad \square$$

Our next aim is to determine the equation of the tooth flanks as involutes of the base curves. We start with the determination of the arc length element of the respective base curve $X_{B,\pm}$. Differentiation of (6.1) with respect to φ under consideration of (3.17), (6.3) and (3.1) yields

$$\begin{aligned}
X'_{B,\pm}(\varphi) &= X'_P(\varphi) \pm e^{\pm i\alpha} \sin \alpha \left(\frac{T'(\varphi)}{\kappa(\varphi)} - \frac{\kappa'(\varphi) T(\varphi)}{\kappa^2(\varphi)} \right) \\
&= X'_P(\varphi) \pm e^{\pm i\alpha} \sin \alpha \left(\frac{i h(\varphi) T(\varphi)}{\kappa(\varphi)} - \frac{\kappa'(\varphi) T(\varphi)}{\kappa^2(\varphi)} \right) \\
&= \left[|X'_P(\varphi)| \pm e^{\pm i\alpha} \sin \alpha \left(i |X'_P(\varphi)| - \frac{\kappa'(\varphi)}{\kappa^2(\varphi)} \right) \right] T(\varphi) \\
&= \left[|X'_P(\varphi)| \pm (\cos \alpha \pm i \sin \alpha) \sin \alpha \left(i |X'_P(\varphi)| - \frac{\kappa'(\varphi)}{\kappa^2(\varphi)} \right) \right] T(\varphi) \\
&= \left[|X'_P(\varphi)| \mp (\cos \alpha \pm i \sin \alpha) \left(\frac{\kappa'(\varphi)}{\kappa^2(\varphi)} - i |X'_P(\varphi)| \right) \sin \alpha \right] T(\varphi) \\
&= \left[|X'_P(\varphi)| \mp \left(\frac{\kappa'(\varphi)}{\kappa^2(\varphi)} \cos \alpha \pm |X'_P(\varphi)| \sin \alpha \right) \sin \alpha \right. \\
&\quad \left. \pm i \left(|X'_P(\varphi)| \cos \alpha \mp \frac{\kappa'(\varphi)}{\kappa^2(\varphi)} \sin \alpha \right) \sin \alpha \right] T(\varphi) \\
&= \left[|X'_P(\varphi)| \mp \frac{\kappa'(\varphi)}{\kappa^2(\varphi)} \cos \alpha \sin \alpha - |X'_P(\varphi)| \sin^2 \alpha \right. \\
&\quad \left. \pm i \left(|X'_P(\varphi)| \cos \alpha \mp \frac{\kappa'(\varphi)}{\kappa^2(\varphi)} \sin \alpha \right) \sin \alpha \right] T(\varphi) \\
&= \left[|X'_P(\varphi)| \cos^2 \alpha \mp \frac{\kappa'(\varphi)}{\kappa^2(\varphi)} \cos \alpha \sin \alpha \right. \\
&\quad \left. \pm i \left(|X'_P(\varphi)| \cos \alpha \mp \frac{\kappa'(\varphi)}{\kappa^2(\varphi)} \sin \alpha \right) \sin \alpha \right] T(\varphi) \\
&= \left[\left(|X'_P(\varphi)| \cos \alpha \mp \frac{\kappa'(\varphi)}{\kappa^2(\varphi)} \sin \alpha \right) \cos \alpha \right. \\
&\quad \left. \pm i \left(|X'_P(\varphi)| \cos \alpha \mp \frac{\kappa'(\varphi)}{\kappa^2(\varphi)} \sin \alpha \right) \sin \alpha \right] T(\varphi)
\end{aligned}$$

$$= \left(|X'_P(\varphi)| \cos \alpha \mp \frac{\kappa'(\varphi)}{\kappa^2(\varphi)} \sin \alpha \right) e^{\pm i\alpha} T(\varphi),$$

hence

$$|X'_{B,\pm}(\varphi)| = \left| |X'_P(\varphi)| \cos \alpha \mp \frac{\kappa'(\varphi)}{\kappa^2(\varphi)} \sin \alpha \right|.$$

Since we do not want to calculate the length of the curve $X_{B,\pm}$, but the length of its developments, it is convenient to use

$$\left(|X'_P(\varphi)| \cos \alpha \mp \frac{\kappa'(\varphi)}{\kappa^2(\varphi)} \sin \alpha \right) d\varphi$$

as length element. This will simplify the calculations. In addition, one avoids the case distinctions that become necessary if $X_{B,\pm}$ has cusps (see Fig. 8.4). We denote by $X_{F,+}^*$ the involute of the base curve $X_{B,+}$ that we obtain when the singular point (cusp) $\varphi_{S,+}$ of $X_{F,+}^*$ is freely chosen in the interval $0 \leq \varphi \leq 2\pi$. Using (2.11) and (2.13), one gets

$$\begin{aligned} X_{F,+}^*(\varphi) &= X_{B,+}(\varphi) + \left[\int_{\varphi}^{\varphi_{S,+}} \left(|X'_P(\varphi)| \cos \alpha - \frac{\kappa'(\varphi)}{\kappa^2(\varphi)} \sin \alpha \right) d\varphi \right] T(\varphi) e^{i\alpha} \\ &= X_{B,+}(\varphi) + \left[a \cos \alpha \int_{\varphi}^{\varphi_{S,+}} \frac{w(\varphi)}{(1 + \psi'(\varphi))^2} d\varphi + \sin \alpha \int_{\varphi}^{\varphi_{S,+}} \left(-\frac{\kappa'(\varphi)}{\kappa^2(\varphi)} \right) d\varphi \right] T(\varphi) e^{i\alpha} \\ &= X_{B,+}(\varphi) + \left[a \cos \alpha I(\varphi, \varphi_{S,+}) + \sin \alpha \left(\frac{1}{\kappa(\varphi_{S,+})} - \frac{1}{\kappa(\varphi)} \right) \right] T(\varphi) e^{i\alpha} \\ &= X_{B,+}(\varphi) - \left[a \cos \alpha I(\varphi_{S,+}, \varphi) - \sin \alpha \left(\frac{1}{\kappa(\varphi_{S,+})} - \frac{1}{\kappa(\varphi)} \right) \right] T(\varphi) e^{i\alpha}. \end{aligned} \quad (6.4)$$

For the involutes $X_{F,-}^*$ of the base curve $X_{B,-}$ we have

$$\begin{aligned} X_{F,-}^*(\varphi) &= X_{B,-}(\varphi) - \left[\int_{\varphi_{S,-}}^{\varphi} \left(|X'_P(\varphi)| \cos \alpha + \frac{\kappa'(\varphi)}{\kappa^2(\varphi)} \sin \alpha \right) d\varphi \right] T(\varphi) e^{-i\alpha} \\ &= X_{B,-}(\varphi) - \left[a \cos \alpha I(\varphi_{S,-}, \varphi) + \sin \alpha \left(\frac{1}{\kappa(\varphi_{S,-})} - \frac{1}{\kappa(\varphi)} \right) \right] T(\varphi) e^{-i\alpha}, \end{aligned} \quad (6.5)$$

where $\varphi_{S,-}$ is the singular point (cusp) of $X_{F,-}^*$. So writing (6.4) and (6.5) together, we have

$$X_{F,\pm}^*(\varphi) = X_{B,\pm}(\varphi) - \left[a \cos \alpha I(\varphi_{S,\pm}, \varphi) \mp \sin \alpha \left(\frac{1}{\kappa(\varphi_{S,\pm})} - \frac{1}{\kappa(\varphi)} \right) \right] T(\varphi) e^{\pm i\alpha}. \quad (6.6)$$

Applying Lemma 6.1 yields

$$\begin{aligned} X_{F,\pm}^*(\varphi) &= X_P(\varphi) \pm \frac{\sin \alpha}{\kappa(\varphi)} T(\varphi) e^{\pm i\alpha} \\ &\quad - \left[a \cos \alpha I(\varphi_{S,\pm}, \varphi) \mp \sin \alpha \left(\frac{1}{\kappa(\varphi_{S,\pm})} - \frac{1}{\kappa(\varphi)} \right) \right] T(\varphi) e^{\pm i\alpha} \\ &= X_P(\varphi) - \left(a \cos \alpha I(\varphi_{S,\pm}, \varphi) \mp \frac{\sin \alpha}{\kappa(\varphi_{S,\pm})} \right) T(\varphi) e^{\pm i\alpha}. \end{aligned}$$

We formulate our result as theorem.

Theorem 6.1. *A parametric equation of the involutes $X_{F,\pm}^*$ of the base curve $X_{B,\pm}$ is given by*

$$X_{F,\pm}^*(\varphi) = X_P(\varphi) - \left(a \cos \alpha I(\varphi_{S,\pm}, \varphi) \mp \frac{\sin \alpha}{\kappa(\varphi_{S,\pm})} \right) T(\varphi) e^{\pm i\alpha},$$

where $\varphi_{S,\pm}$ is the value of φ at the singular point of $X_{F,\pm}^*$, I is the integral (2.13), and κ and T are the curvature (3.21) and the tangent unit vector (3.1), respectively, of the centrode X_P .

It should be emphasized that $\kappa(\varphi_{S,\pm})$ in Theorem 6.1 is the curvature of the **centrode** X_P at the singular point $\varphi_{S,\pm}$ of the **involute** $X_{F,\pm}^*$.

It remains to be shown that the involutes obtained in this way are indeed the tooth flanks according to Theorem 3.1 (cf. the quote at the beginning of this section). This will be proved in the following corollary.

Corollary 6.1. *The flank curve $X_{F,k,\pm}$, $k \in \{1, \dots, z_1\}$, generated with the rack-cutter is identical to the involute $X_{F,k,\pm}^*$ of the base curve $X_{B,\pm}$ whose parametric equation is*

$$X_{F,k,\pm}^*(\varphi) = X_P(\varphi) - \left(a \cos \alpha I(\varphi_{S,k,\pm}, \varphi) \mp \frac{\sin \alpha}{\kappa(\varphi_{S,k,\pm})} \right) T(\varphi) e^{\pm i\alpha}.$$

Proof. The midpoint of tooth k on the centrode X_P is given by $X_P(\chi(k))$ with $\chi(k)$ according to (3.3). Condition (5.4) for the value $\varphi_{S,k,\pm}$ of φ at the singular point of the flank $X_{F,k,\pm}$ states that

$$\lambda_{k,\pm}(\varphi_{S,k,\pm}) \cos \alpha = \pm \frac{\sin \alpha}{\kappa(\varphi_{S,k,\pm})}.$$

Using (3.4), it follows that

$$\begin{aligned} X_{F,k,\pm}^*(\varphi) &= X_P(\varphi) - \left(a \cos \alpha I(\varphi_{S,k,\pm}, \varphi) \mp \frac{\sin \alpha}{\kappa(\varphi_{S,k,\pm})} \right) T(\varphi) e^{\pm i\alpha} \\ &= X_P(\varphi) - \left[a \cos \alpha I(\varphi_{S,k,\pm}, \varphi) \mp (\pm \lambda_{k,\pm}(\varphi_{S,k,\pm}) \cos \alpha) \right] T(\varphi) e^{\pm i\alpha} \\ &= X_P(\varphi) - \left[a I(\varphi_{S,k,\pm}, \varphi) - \lambda_{k,\pm}(\varphi_{S,k,\pm}) \right] T(\varphi) e^{\pm i\alpha} \cos \alpha \\ &= X_P(\varphi) - \left[a I(\varphi_{S,k,\pm}, \varphi) \mp \frac{\pi m}{4} + a I(\chi(k), \varphi_{S,k,\pm}) \right] T(\varphi) e^{\pm i\alpha} \cos \alpha \\ &= X_P(\varphi) - \left[\mp \frac{\pi m}{4} + a (I(\chi(k), \varphi_{S,k,\pm}) + I(\varphi_{S,k,\pm}, \varphi)) \right] T(\varphi) e^{\pm i\alpha} \cos \alpha \\ &= X_P(\varphi) + \left(\pm \frac{\pi m}{4} - a I(\chi(k), \varphi) \right) T(\varphi) e^{\pm i\alpha} \cos \alpha \\ &= X_P(\varphi) + \lambda_{k,\pm}(\varphi) T(\varphi) e^{\pm i\alpha} \cos \alpha. \end{aligned}$$

One sees that the last line is identical to the parametric equation $X_{F,k,\pm}(\varphi)$ of $X_{F,k,\pm}$ in Theorem 3.1. \square

The following corollary is important for the calculation, or at least estimation, of the tooth flank pressure by means of the Hertzian theory.

Corollary 6.2. *The radius of curvature at point φ of the involute $X_{F,k,\pm}^* \equiv X_{F,k,\pm}$ is given by*

$$\left| a \cos \alpha I(\varphi_{S,k,\pm}) \mp \sin \alpha \left(\frac{1}{\kappa(\varphi_{S,k,\pm}, \varphi)} - \frac{1}{\kappa(\varphi)} \right) \right|.$$

Proof. Since $X_{B,\pm}$ is the evolute of the involutes $X_{F,k,\pm}^*$, from (6.6) it is known that

$$- \left[a \cos \alpha I(\varphi_{S,k,\pm}, \varphi) \mp \sin \alpha \left(\frac{1}{\kappa(\varphi_{S,k,\pm})} \mp \frac{1}{\kappa(\varphi)} \right) \right]$$

is the signed radius of curvature at point $X_{F,k,\pm}^*(\varphi)$ of $X_{F,k,\pm}^*$. The proposition of Corollary 6.2 follows immediately. \square

6.2 Base curve of the driven gear

Lemma 6.2. *A parametric equation of the base curves $\Xi_{B,\pm}$ of the driven gear is given by*

$$\Xi_{B,\pm}(\varphi) = \Xi_P(\varphi) \pm \frac{\sin \alpha}{\tilde{\kappa}(\varphi)} \tilde{T}(\varphi) e^{\pm i\alpha}, \quad 0 \leq \varphi \leq 2\pi, \quad (6.7)$$

where $\tilde{\kappa}(\varphi)$ and $\tilde{T}(\varphi)$ are the curvature and the tangent unit vector, respectively, of the centrode Ξ_P at point φ .

Proof. The two straight lines that intersect the centrode Ξ_P at point φ with the angles $-\alpha$ and $+\alpha$, respectively, are given by

$$\Xi = \Xi_P(\varphi) + \mu \tilde{T}(\varphi) e^{\pm i\alpha}, \quad \mu \in \mathbb{R}.$$

The proof is now analogous to that of Lemma 6.1. \square

Theorem 6.2. *A parametric equation of the involutes $\Xi_{F,\pm}^*$ of the base curve $\Xi_{B,\pm}$ is given by*

$$\Xi_{F,\pm}^*(\varphi) = \Xi_P(\varphi) - \left(a \cos \alpha I(\varphi_{S,\pm}, \varphi) \mp \frac{\sin \alpha}{\tilde{\kappa}(\varphi_{S,\pm})} \right) \tilde{T}(\varphi) e^{\pm i\alpha},$$

where $\varphi_{S,\pm}$ is value of φ at the singular point of $\Xi_{F,\pm}^*$, I is the integral (2.13), and $\tilde{\kappa}$ and \tilde{T} are the curvature (4.14) and the tangent unit vector (4.2), respectively, of the centrode Ξ_P .

Proof. The proof is analogous to that of Theorem 6.1. \square

Corollary 6.3. *The flank curve $\Xi_{F,k,\pm}$, $k \in \{1, \dots, z_2\}$, generated with the rack-cutter is identical to the involute $\Xi_{F,k,\pm}^*$ of the base curve $\Xi_{B,\pm}$ whose parametric equation is*

$$\Xi_{F,k,\pm}^*(\varphi) = \Xi_P(\varphi) - \left(a \cos \alpha I(\varphi_{S,k,\pm}, \varphi) \mp \frac{\sin \alpha}{\tilde{\kappa}(\tilde{\varphi}_{S,k,\pm})} \right) \tilde{T}(\varphi) e^{\pm i\alpha},$$

where $\tilde{\varphi}_{S,k,\pm}$ is the value of φ at the singular point of $\Xi_{F,k,\pm}$.

Proof. The midpoint of tooth k on the centrode Ξ_P is given by $\Xi_P(\chi(k))$ with $\chi(k)$ according to (3.3). Condition (5.11) for the value $\tilde{\varphi}_{S,k,\pm}$ of φ at the singular point of the flank $\Xi_{F,k,\pm}$ states that

$$\lambda_{k,\pm}(\tilde{\varphi}_{S,k,\pm}) \cos \alpha = \pm \frac{\sin \alpha}{\tilde{\kappa}(\tilde{\varphi}_{S,k,\pm})}.$$

Using (3.4), it follows that

$$\begin{aligned} \Xi_{F,k,\pm}^*(\varphi) &= \Xi_P(\varphi) - \left(a \cos \alpha I(\tilde{\varphi}_{S,k,\pm}, \varphi) \mp \frac{\sin \alpha}{\tilde{\kappa}(\tilde{\varphi}_{S,k,\pm})} \right) \tilde{T}(\varphi) e^{\pm i\alpha} \\ &= \Xi_P(\varphi) - [a \cos \alpha I(\tilde{\varphi}_{S,k,\pm}, \varphi) \mp (\pm \lambda_{k,\pm}(\tilde{\varphi}_{S,k,\pm}) \cos \alpha)] \tilde{T}(\varphi) e^{\pm i\alpha} \\ &= \Xi_P(\varphi) - [a I(\tilde{\varphi}_{S,k,\pm}, \varphi) - \lambda_{k,\pm}(\tilde{\varphi}_{S,k,\pm})] \tilde{T}(\varphi) e^{\pm i\alpha} \cos \alpha \\ &= \Xi_P(\varphi) - \left[a I(\tilde{\varphi}_{S,k,\pm}, \varphi) \mp \frac{\pi m}{4} + a I(\chi(k), \tilde{\varphi}_{S,k,\pm}) \right] \tilde{T}(\varphi) e^{\pm i\alpha} \cos \alpha \\ &= \Xi_P(\varphi) - \left[\mp \frac{\pi m}{4} + a (I(\chi(k), \tilde{\varphi}_{S,k,\pm}) + I(\tilde{\varphi}_{S,k,\pm}, \varphi)) \right] \tilde{T}(\varphi) e^{\pm i\alpha} \cos \alpha \\ &= \Xi_P(\varphi) + \left(\pm \frac{\pi m}{4} - a I(\chi(k), \varphi) \right) \tilde{T}(\varphi) e^{\pm i\alpha} \cos \alpha \\ &= \Xi_P(\varphi) + \lambda_{k,\pm}(\varphi) \tilde{T}(\varphi) e^{\pm i\alpha} \cos \alpha. \end{aligned}$$

One sees that the last line is identical to the parametric equation $\Xi_{F,k,\pm}(\varphi)$ of $\Xi_{F,k,\pm}$ in Theorem 4.1. \square

7 Algorithm

For both gears:

1. Assume that the center distance a is equal to 1, and check that the centrode c_1 of the drive gear and the centrode c_2 of the driven gear are both convex curves.
2. Evaluate the integral $I(0, 2\pi)$ (see (2.13)); if necessary, numerically.
3. Choose the module m and the number z_1 of teeth of the drive gear, and calculate the center distance with (2.14).
4. Choose angle α , addendum h_a , dedendum h_f and fillet radius ρ (see Fig. 2.2).

For the drive gear:

5. Determine the values $\chi(k)$, $k = 1, 2, \dots, z_1$, of the parameter (drive angle) φ from (3.3). (These values divide X_P into arcs of equal length $p = \pi m$. $\chi(k)$ is the value for the mid of tooth k .)
6. Determine the values $\varphi_{S,k,\pm}$, $k = 1, 2, \dots, z_1$, of φ at the singular points of the involutes $X_{F,k,\pm} \equiv X_{F,k,\pm}^*$ with (5.2).
7. Check each tooth flank for the occurrence of undercut with (5.5). Alternatively, the parameters of the gear can be specified using inequality (5.6) so that no undercut occurs at all.
8. Perform the calculations of this step for each “-”-flank.

If the flank has undercut, then determine the values $\varphi_{F,k,-,1}$ and $\varphi_{A,k,-,1}$ of the angle φ as solution of

$$X_{F,k,-}(\varphi_{F,k,-,1}) = X_{\varrho,k,-}(\varphi_{A,k,-,1}) \quad (7.1)$$

where $X_{F,k,-}(\varphi)$ and $X_{\varrho,k,-}(\varphi)$ are given by (3.7) and (3.29), respectively. If the flank is free of undercut, then $\varphi_{F,k,-,1} = \varphi_{A,k,-,1} = \varphi_{B,k,-}$ and the value $\varphi_{B,k,-}$ of φ is obtained as solution of (5.3).

Determine the value $\varphi_{A,k,-,2}$ of the angle φ as solution of (3.30). Determine the values $\varphi_{F,k,-,2}$ and $\varphi_{p,k,+,1}$ of the angle φ as solution of

$$X_{F,k,-}(\varphi_{F,k,-,2}) = X_a(\varphi_{p,k,+,1}) \quad (7.2)$$

with $X_a(\varphi) := X_{p,h_a,+}(\varphi)$ ($X_{p,d,\pm}(\varphi)$ see (3.25)). The “-”-flank of tooth k is then given by

$$X = \begin{cases} X_{\varrho,k,-}(\varphi), & \varphi_{A,k,-,1} \leq \varphi \leq \varphi_{A,k,-,2}, \\ X_{F,k,-}(\varphi), & \varphi_{F,k,-,1} \leq \varphi \leq \varphi_{F,k,-,2}. \end{cases} \quad (7.3)$$

9. Perform the calculations of this step for each “+”-flank.

If the flank has undercut, then determine the values $\varphi_{F,k,+,2}$ and $\varphi_{A,k,+,2}$ of the angle φ as solution of

$$X_{F,k,+}(\varphi_{F,k,+,2}) = X_{\varrho,k,+}(\varphi_{A,k,+,2}) \quad (7.4)$$

where $X_{F,k,+}(\varphi)$ and $X_{\varrho,k,+}(\varphi)$ are given by (3.7) and (3.29), respectively. If the flank is free of undercut, then $\varphi_{F,k,+,2} = \varphi_{A,k,+,2} = \varphi_{B,k,+}$ and the value $\varphi_{B,k,+}$ of φ is obtained as solution of (5.3).

Determine the values $\varphi_{F,k,+,1}$ and $\varphi_{p,k,+,2}$ of the angle φ as solution of

$$X_{F,k,+}(\varphi_{F,k,+,1}) = X_a(\varphi_{p,k,+,2}). \quad (7.5)$$

Determine the value $\varphi_{A,k,+,1}$ of the angle φ as solution of (3.31). The “+”-flank of tooth k is then given by

$$X = \begin{cases} X_{F,k,+}(\varphi), & \varphi_{F,k,+,1} \leq \varphi \leq \varphi_{F,k,+,2}, \\ X_{\varrho,k,+}(\varphi), & \varphi_{A,k,+,1} \leq \varphi \leq \varphi_{A,k,+,2}. \end{cases} \quad (7.6)$$

10. The arc of the addendum curve X_a for tooth k , $k = 1, \dots, z_1$, is given by

$$X = X_a(\varphi), \quad \varphi_{p,k,+,1} \leq \varphi \leq \varphi_{p,k,+,2}, \quad (7.7)$$

with $\varphi_{p,k,+,1}$ from Step 8.

11. The arc of the dedendum curve X_f between tooth k , $k = 1, \dots, z_1 - 1$, and tooth $k + 1$ is given by

$$X = X_f(\varphi), \quad \varphi_{A,k,+,1} \leq \varphi \leq \varphi_{A,k+1,-,2}. \quad (7.8)$$

The arc of the dedendum curve X_f between tooth z_1 and tooth 1 is given by

$$X = X_f(\varphi), \quad \varphi_{A,z_1,+,1} \leq \varphi \leq 2\pi + \varphi_{A,1,-,2}. \quad (7.9)$$

For the driven gear:

12. Determine the values $\chi(k)$, $k = 1, 2, \dots, z_2$, of φ from (3.3). Since $\chi(1), \dots, \chi(z_1)$ are already known from Step 5, performing this step is only necessary to determine $\chi(z_1 + 1), \dots, \chi(z_2)$ if $z_2 > z_1$.
13. Determine the values $\tilde{\varphi}_{S,k,\pm}$, $k = 1, 2, \dots, z_2$, of φ at the singular points of the involutes $\Xi_{F,k,\pm} \equiv \Xi_{F,k,\pm}^*$ with (5.11).
14. Check each tooth flank for the occurrence of undercut with (5.13). Alternatively, the parameters of the gear can be specified using inequality (5.14) so that no undercut occurs at all.
15. Perform the calculations of this step for each “-”-flank.

If the flank has undercut, then determine the values $\tilde{\varphi}_{F,k,-,2}$ and $\tilde{\varphi}_{A,k,-,2}$ and of the angle φ as solution of

$$\Xi_{F,k,-}(\tilde{\varphi}_{F,k,-,2}) = \Xi_{\varrho,k,-}(\tilde{\varphi}_{A,k,-,2}) \quad (7.10)$$

where $\Xi_{F,k,-}(\varphi)$ and $\Xi_{\varrho,k,-}(\varphi)$ are given by (4.6) and (4.18), respectively. If the flank is free of undercut, then $\tilde{\varphi}_{F,k,-,2} = \tilde{\varphi}_{A,k,-,2} = \tilde{\varphi}_{B,k,-}$ and the value $\tilde{\varphi}_{B,k,-}$ of φ is obtained as solution of (5.12).

Determine the value $\tilde{\varphi}_{A,k,-,1}$ of the angle φ as solution of (4.19). Determine the values $\tilde{\varphi}_{F,k,-,1}$ and $\tilde{\varphi}_{p,k,+,1}$ of the angle φ as solution of

$$\Xi_{F,k,-}(\tilde{\varphi}_{F,k,-,1}) = \Xi_a(\tilde{\varphi}_{p,k,+,1}) \quad (7.11)$$

with $\Xi_a(\varphi) \equiv \Xi_{p,h_a,+}(\varphi)$ ($\Xi_{p,d,\pm}(\varphi)$ see (4.15)). The “-”-flank of tooth space k is then given by

$$\Xi = \begin{cases} \Xi_{F,k,-}(\varphi), & \tilde{\varphi}_{F,k,-,1} \leq \varphi \leq \tilde{\varphi}_{F,k,-,2}, \\ \Xi_{\varrho,k,-}(\varphi), & \tilde{\varphi}_{A,k,-,1} \leq \varphi \leq \tilde{\varphi}_{A,k,-,2}. \end{cases} \quad (7.12)$$

16. Perform the calculations of this step for each “+”-flank.

If the flank has undercut, then determine the values $\tilde{\varphi}_{F,k,+,1}$ and $\tilde{\varphi}_{A,k,+,1}$ of the angle φ as solution of

$$\Xi_{F,k,+}(\tilde{\varphi}_{F,k,+,1}) = \Xi_{\varrho,k,+}(\tilde{\varphi}_{A,k,+,1}) \quad (7.13)$$

where $\Xi_{F,k,+}(\varphi)$ and $\Xi_{\varrho,k,+}(\varphi)$ are given by (4.6) and (4.18), respectively. If the flank is free of undercut, then $\tilde{\varphi}_{F,k,+,1} = \tilde{\varphi}_{A,k,+,1} = \tilde{\varphi}_{B,k,+}$ and the value $\tilde{\varphi}_{B,k,+}$ of φ is obtained as solution of (5.12).

Determine the value $\tilde{\varphi}_{A,k,+,2}$ of the angle φ as solution of (4.19). Determine the values $\tilde{\varphi}_{F,k,+,2}$ and $\tilde{\varphi}_{p,k,+,2}$ of the angle φ as solution of

$$\Xi_{F,k,+}(\tilde{\varphi}_{F,k,+,2}) = \Xi_a(\tilde{\varphi}_{p,k,+,2}). \quad (7.14)$$

The “+”-flank of tooth space k is then given by

$$\Xi = \begin{cases} \Xi_{F,k,+}(\varphi), & \tilde{\varphi}_{F,k,+,1} \leq \varphi \leq \tilde{\varphi}_{F,k,+,2}, \\ \Xi_{\varrho,k,+}(\varphi), & \tilde{\varphi}_{A,k,+,1} \leq \varphi \leq \tilde{\varphi}_{A,k,+,2}. \end{cases} \quad (7.15)$$

17. The arc of the dedendum curve Ξ_f of tooth space k , $k = 1, \dots, z_2$, is given by

$$\Xi = \Xi_f(\varphi), \quad \tilde{\varphi}_{A,k,-,1} \leq \varphi \leq \tilde{\varphi}_{A,k,+,2}. \quad (7.16)$$

18. The arc of the addendum curve Ξ_a between tooth space k , $k = 1, \dots, z_2 - 1$, and tooth space $k + 1$ is given by

$$\Xi = \Xi_a(\varphi), \quad \tilde{\varphi}_{p,k,+,2} \leq \varphi \leq \tilde{\varphi}_{p,k+1,+,1}. \quad (7.17)$$

The arc of the addendum curve Ξ_a between tooth space z_2 and tooth space 1 is given by

$$\Xi = \Xi_a(\varphi), \quad \tilde{\varphi}_{p,z_2,+,2} \leq \varphi \leq 2\pi + \tilde{\varphi}_{p,1,+,1}. \quad (7.18)$$

For the fast numerical solution of the occurring equations, e.g. (3.3) and (7.1), one can use the one-dimensional or two-dimensional Newton’s method, respectively.

8 Example

Let the transmission funktion given by

$$\psi(\varphi) = \varphi - b \sin \varphi, \quad 0 \leq \varphi \leq 2\pi, \quad b = \text{const} \in \mathbb{R}.$$

Note that $\psi(2\pi) = 2\pi$.

We consider the centrod X_P of the drive gear. From (2.7) it follows that X_P has the polar equation

$$r(\varphi) = \frac{1 - b \cos \varphi}{2 - b \cos \varphi} a.$$

We assume $a = 1$. Considering Fig. 8.1, one sees that not every value of b results in a practically usable centrod X_P . Since the teeth are to be generated with a rack-cutter, only centrodes with curvature $\kappa(\varphi) \leq 0$ for $0 \leq \varphi \leq 2\pi$ come into question. In order to avoid gears with exotic shapes, only centrodes without self-intersections should be used. A small investigation shows that $2 - \sqrt{2} \approx 0.585786$ is the biggest value of b with $\kappa(\varphi) \leq 0$ for $0 \leq \varphi \leq 2\pi$, and $\max_{0 \leq \varphi \leq 2\pi} \kappa(\varphi) = 0 = \kappa(0) = \kappa(2\pi)$. For the centrod Ξ_P of the driven gear one finds $\tilde{\kappa}(\varphi) > 0$ for $b = 2 - \sqrt{2}$ and $0 \leq \varphi \leq 2\pi$. So in the following we use $b = 2 - \sqrt{2}$. The graph of $\psi(\varphi)$ is shown in Fig. 8.2. Our transmission funktion is – up to a phase difference of π – equal to the transmission funktion shown in [8, Fig. 18 b].

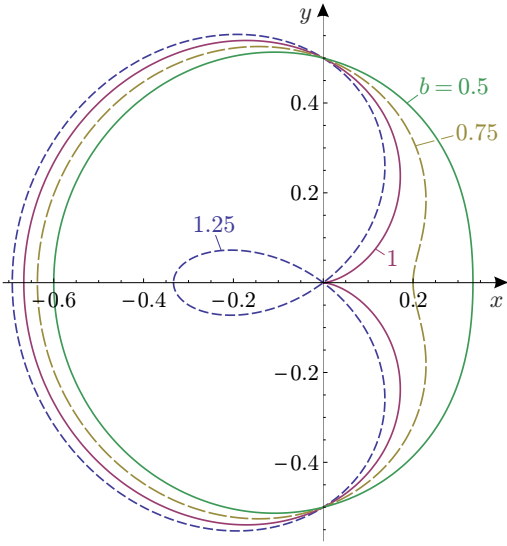


Fig. 8.1: The centre X_P with $a = 1$ and different values of the parameter b

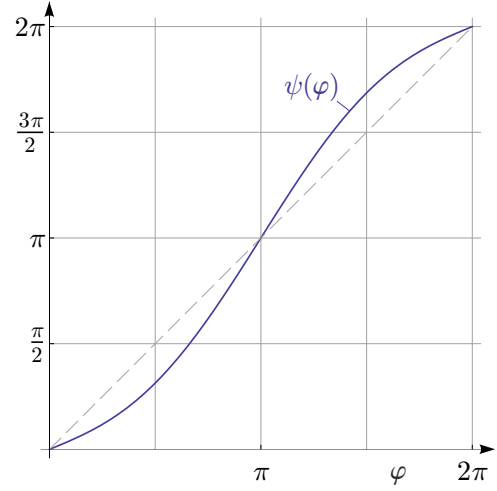


Fig. 8.2: Graph of $\psi(\varphi)$ with $b = 2 - \sqrt{2}$

Table 8.1: Values of $\chi(k)$

k	1	2	3	4	5	6	7
$\chi(k)$	0	0.674065	1.18877	1.63010	2.03297	2.41317	2.78037
k	8	9	10	11	12	13	14
$\chi(k)$	π	3.50282	3.87002	4.25022	4.65309	5.09441	5.60912

A numerical evaluation yields $I(0, 2\pi) \approx 3.09315$ ($I(\varphi_0, \varphi_1)$ see (2.13)). Choosing $m = 2$ and $z_1 = 14$, from (2.14) we get $a \approx 28.4385$. The centres X_P and Ξ_P with this value of a are to be seen in Fig. 8.3 (cp. the centres in [8, Fig. 18 a]).

From (3.3) we get the values $\chi(1), \dots, \chi(14)$ in Table 8.1.

After choosing $h_a = m = 2$, $h_f = 1.2 \cdot m = 2.4$ and $\varrho = 0.3 \cdot m = 0.6$ (h_a, h_f, ϱ see Fig. 2.2), we get the pair of gears in Fig. 8.3.

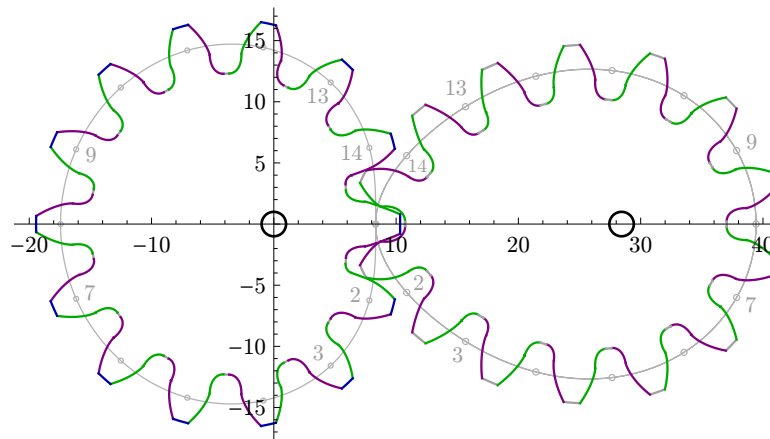


Fig. 8.3: Example with $\psi(\varphi) = \varphi - (2 - \sqrt{2}) \sin \varphi$ and $z_1 = 14 = z_2$

Table 8.2 shows the values $\varphi_{S,k,\pm}$ of φ at the singular points of $X_{F,k,\pm}$ and the curvatures $\kappa(\varphi_{S,k,\pm})$ of X_P at $\varphi_{S,k,\pm}$ for the drive gear. From (5.5) we get $-\kappa(\varphi_{S,k,\pm}) \leq 0.0583369$ as condition for non-undercutting. So one sees that only the “-”-flank of tooth 2, and the “+”-flank

of tooth 14 are free of undercut. (The curves of tooth 14 are shown in Fig. 3.2.)

Table 8.2: Drive gear: Singular points $\varphi_{S,k,\pm}$, curvatures $\kappa(\varphi_{S,k,\pm})$ and undercut (UC)

k	$\varphi_{S,k,-}$	$\kappa(\varphi_{S,k,-})$	UC	$\varphi_{S,k,+}$	$\kappa(\varphi_{S,k,+})$	UC
1	-0.662309	-0.0793920	•	0.662309	-0.0793920	•
2	-0.370208	-0.0459235	–	1.13773	-0.0902213	•
3	0.697105	-0.0816165	•	1.60927	-0.0827132	•
4	1.23593	-0.0892922	•	2.04386	-0.0744589	•
5	1.64804	-0.0819279	•	2.44631	-0.0690331	•
6	2.02344	-0.0748006	•	2.82554	-0.0662394	•
7	2.38300	-0.0697165	•	3.18979	-0.0655454	•
8	2.73727	-0.0666956	•	3.54591	-0.0666956	•
9	3.09339	-0.0655454	•	3.90019	-0.0697165	•
10	3.45764	-0.0662394	•	4.25974	-0.0748006	•
11	3.83688	-0.0690331	•	4.63514	-0.0819279	•
12	4.23933	-0.0744589	•	5.04725	-0.0892922	•
13	4.67392	-0.0827132	•	5.58608	-0.0816165	•
14	5.14546	-0.0902213	•	6.65339	-0.0459235	–

Fig. 8.4 shows for the drive gear the centrod X_P , the base curve (evolute) $X_{B,+}$, the involutes $X_{F,k,+}$, $k = 1, \dots, 14$, and for comparison the involute $X_{F,14,-}$. The base curve has one cusp and one point at infinity. The point at infinity occurs for $\varphi = 0$ and is caused by the fact that the straight lines whose envelope is the base curve have no intersection in the finite for $\varphi = 0$. Note that the base curve $X_{B,-}$ and all involutes $X_{F,k,-}$ are obtained by mirroring the corresponding “+”-curves on the abscissa. For example, $X_{F,14,-}$ corresponds to $X_{F,2,+}$.

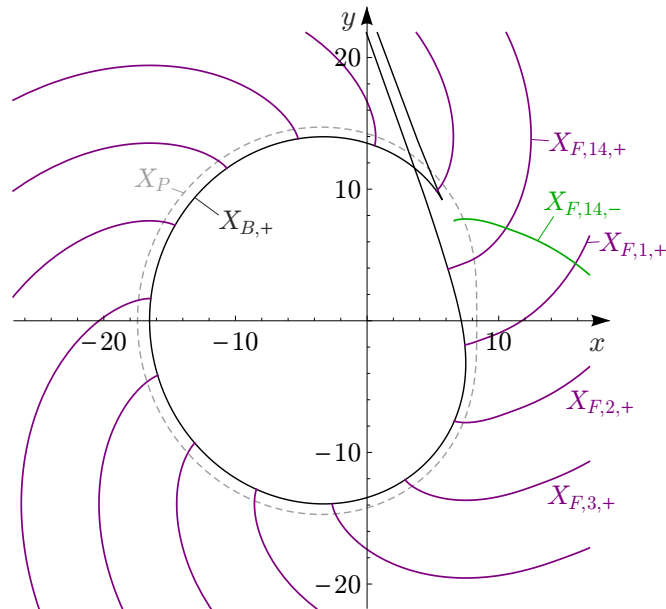


Fig. 8.4: Centrod X_P (dashed), base curve $X_{B,+}$ and involutes of the drive gear

A Appendix: The exterior product

The *exterior product* (see Luck and Modler [11, p. 414]) of two complex numbers $A = x_A + iy_A$ and $B = x_B + iy_B$ is a real number, and is defined by

$$[A, B] = \frac{i}{2} (A \bar{B} - \bar{A} B) = x_A y_B - y_A x_B. \quad (\text{A.1})$$

The real number $[A, B]$ is the signed area of the parallelogram spanned by the complex vectors A and B . The exterior product is

$$\left. \begin{array}{l} \text{anticommutative:} \quad [A, B] = -[B, A], \\ \text{distributive over addition:} \quad [A + B, C] = [A, C] + [B, C], \\ \text{not associative:} \quad [[A, B], C] \neq [A, [B, C]]. \end{array} \right\} \quad (\text{A.2})$$

Further rules:

$$[1, A] = \text{Im } A, \quad (\text{A.3})$$

$$[A, Bc] = [Ac, B] = c[A, B], \quad c \in \mathbb{R}, \quad (\text{A.4})$$

$$[AC, BC] = [AC\bar{C}, B] = C\bar{C}[A, B]. \quad (\text{A.5})$$

If A and B are functions of a real parameter φ , then

$$\begin{aligned} [A(\varphi), B(\varphi)]' &\equiv \frac{d}{d\varphi} [A(\varphi), B(\varphi)] = \frac{i}{2} (A' \bar{B} + A \bar{B}' - \bar{A}' B - \bar{A} B') \\ &= \frac{i}{2} (A' \bar{B} - \bar{A}' B) + \frac{i}{2} (A \bar{B}' - \bar{A} B') \\ &= [A'(\varphi), B(\varphi)] + [A(\varphi), B'(\varphi)] \quad (\text{product rule}). \end{aligned} \quad (\text{A.6})$$

Clearly, three points A, B, X lie on a straight line g if

$$[A - X, B - X] = 0.$$

From this equation we get

$$\begin{aligned} 0 &= [A, B - X] - [X, B - X] = [A, B] - [A, X] - [X, B] + \underbrace{[X, X]}_0 \\ &= [A, B] - ([A, X] - [B, X]) = [A, B] - [A - B, X], \end{aligned}$$

hence

$$[A - B, X] = [A, B]. \quad (\text{A.7})$$

If X is an arbitrary point of g , Eq. (A.7) can be considered as the equation of the line through the points A and B .

B Appendix: Formula symbols

a	center distance \rightarrow Fig. 2.1, (2.14)
B	contact point of $X_{F,k,\pm}$ and $X_{\varrho,k,\pm} \rightarrow$ (5.3)
\mathbb{C}	set of complex numbers \rightarrow (2.8), (2.9)

C_{\pm}	point of the rack-cutter → Figures 2.2 and 3.4
D_{\pm}	point of the rack-cutter → Figures 2.2 and 5.1
$h(\varphi)$	auxiliary function → (3.16), (3.19)
$\tilde{h}(\varphi)$	auxiliary function → (4.10)
h_a	addendum of the gear teeth, dedendum of the rack-cutter teeth → Fig. 2.2
h_f	dedendum of the gear teeth, addendum of the rack-cutter teeth → Fig. 2.2
h_f^*	factor → (5.7)
$I(\varphi_0, \varphi_1)$	integral → (2.13)
i	imaginary unit, $i^2 = -1$
ℓ_1	distance → Figures 2.2 and 3.4
ℓ_2	distance → Figures 2.2 and 3.4
ℓ_3	distance → Figures 2.2 and 5.1
ℓ_4	distance → Figures 2.2 and 5.1
M_{\pm}	mid point of the fillet of the rack-cutter “ \pm ”-flank → Fig. 2.2
m	module → Fig. 2.2, (2.14)
$N_{M,k,\pm}(\varphi)$	normal unit vector at point $X_{M,k,\pm}(\varphi)$ of the mid point curve $X_{M,k,\pm}$ → (3.28)
$\tilde{N}_{M,k,\pm}(\varphi)$	normal unit vector at point $\Xi_{M,k,\pm}(\varphi)$ of the mid point curve $\Xi_{M,k,\pm}$ → (4.17)
O_1	pivot point of the drive gear → Fig. 2.1
O_2	pivot point of the driven gear → Fig. 2.1
P	pitch point, instantaneous center of relative rotation of drive and driven gear → Fig. 2.1
p	tooth pitch $p = \pi m$ → Fig. 2.2
\mathbb{R}	set of real numbers
$R(\varphi)$	distance between O_2 and P → Fig. 2.1, (2.7)
$r(\varphi)$	distance between O_1 and P → Fig. 2.1, (2.7)
R_1	point of the rack-cutter that coincides with $X_P(\chi(k))$ for $\varphi = \chi(k)$ when the tooth k of the driving gear is generated → Fig. 2.2
R_2	point of the rack-cutter that coincides with $\Xi_P(\chi(k))$ for $\varphi = \chi(k)$ when the tooth space k of the driven gear is generated → Fig. 2.2
S	singularity of $X_{F,k,\pm}$ → (5.2)
$s(\varphi_0, \varphi_1)$	arc length between points φ_0 and φ_1 → (2.10)
t	time → (2.6)
$T(\varphi)$	tangent unit vector at point $X_P(\varphi)$ of X_P → (3.1)
t_x	real part of $T(\varphi)$ → (3.2)
t_y	imaginary part of $T(\varphi)$ → (3.2)
$\tilde{T}(\varphi)$	tangent unit vector at point $\Xi(\varphi)$ of Ξ_P → (4.2)
t_{ξ}	real part of $\tilde{T}(\varphi)$ → (4.3)
t_{η}	imaginary part of $\tilde{T}(\varphi)$ → (4.3)
$w(\varphi)$	auxiliary function → (2.12)
X_a	addendum curve of the drive gear: $X_a := X_{p,h_a,+}$ → Fig. 3.2, (3.25)
$X_{B,\pm}(\varphi)$	parametric equation of the bases curves (evolutes) $X_{B,\pm}$ for the flank curves (involute) “+” and “-” of the drive gear → (6.1)
$X_{F,k,\pm}(\varphi)$	parametric equation of the flank curves $X_{F,k,\pm}$ of the tooth k (see Fig. 3.2) of the drive gear → (3.7)
$x_{F,k,\pm}(\varphi)$	real part of $X_{F,k,\pm}(\varphi)$ → Corollary 3.1

$X_{F,\pm}^*(\varphi)$	parametric equation of the involutes $X_{F,\pm}^*$ of the base curve $X_{B,\pm}$ → Theorem 6.1
X_f	dedendum curve of the drive gear: $X_f := X_{p,h_f,-}$ → Fig. 3.2, (3.25)
$X_{M,k,\pm}(\varphi)$	parametric equations of the curves $X_{M,k,+}$ and $X_{M,k,-}$ (see Fig. 3.2) of the points M_+ and M_- , respectively, in Fig. 2.2 → (3.27)
$X_P(\varphi)$	parametric equation of the centrode X_P of the drive gear → (2.8), Fig. 2.1
$X_{p,d,\pm}(\varphi)$	parametric equations of an outer (“+”) and inner (“-”) parallel curve of X_P with distance d → (3.25)
$X_{W,k,\pm}(\varphi, \mu)$	parametric equations of the rack-cutter flank lines for the generation of tooth k of the drive gear → (3.5) (for the definition of “+” and “-” see Fig. 2.2)
$x_{W,k,\pm}(\varphi, \mu)$	real part $X_{W,k,\pm}(\varphi, \mu)$ → (3.6)
$X_{\rho,k,\pm}(\varphi)$	parametric equations of the parallel curves (fillets) $X_{\rho,k,\pm}$ (see Fig. 3.2) of $X_{M,k,\pm}$ with distance ρ → (3.29)
$y_{F,k,\pm}(\varphi)$	imaginary part of $X_{F,k,\pm}(\varphi)$ → Corollary 3.1
$y_{W,k,\pm}(\varphi, \mu)$	imaginary part of $X_{W,k,\pm}(\varphi, \mu)$ → (3.6)
z_1	number of teeth of the drive gear → (2.14)
z_2	number of teeth of the driven gear
α	rack-cutter profile angle → Fig. 2.2
γ	rotation angle of the driven gear → Fig. 2.1, (2.3)
$\eta_{F,k,\pm}(\varphi)$	imaginary part of $\Xi_{F,k,\pm}(\varphi)$ → Corollary 4.1
$\eta_{W,k,\pm}(\varphi, \mu)$	imaginary part $\Xi_{W,k,\pm}(\varphi, \mu)$ → (4.5)
$\kappa(\varphi)$	curvature at point φ of X_P → (3.21)
$\tilde{\kappa}(\varphi)$	curvature at point φ of Ξ_P → (4.14)
$\lambda_{k,\pm}(\varphi)$	auxiliary function → (3.4)
Ξ_a	addendum curve of the driven gear: $\Xi_a := \Xi_{p,h_a,+}$, (4.15)
$\Xi_{B,\pm}(\varphi)$	parametric equation of the base curves (evolutes) $\Xi_{B,\pm}$ for the flank curves (involutes) “+” and “-” of the driven gear → (6.7)
$\Xi_{F,k,\pm}(\varphi)$	parametric equations of the flank curves $\Xi_{F,k,\pm}$ of the tooth space k of the driven gear → (4.6)
$\xi_{F,k,\pm}(\varphi)$	real part of $\Xi_{F,k,\pm}(\varphi)$ → Corollary 4.1
$\Xi_{F,\pm}^*(\varphi)$	parametric equation of the involutes $\Xi_{F,\pm}^*$ of the base curve $\Xi_{B,\pm}$ → Theorem 6.2
Ξ_f	dedendum curve of the driven gear: $\Xi_f := \Xi_{p,h_f,-}$, (4.15)
$\Xi_{M,k,\pm}(\varphi)$	parametric equation of the curves $\Xi_{M,k,\pm}$ of the points M_+ and M_- , respectively, in Fig. 2.2 → (4.16)
$\Xi_P(\varphi)$	parametric equation of the centrode Ξ_P of the driven gear → (2.9), Fig. 2.1
$\Xi_{p,d,\pm}(\varphi)$	parametric equation of an outer (“+”) and inner (“-”) parallel curve of Ξ_P with distance d → (4.15)
$\Xi_{W,k,\pm}(\varphi, \mu)$	parametric equation of the rack-cutter flanks for the generation of tooth space k of the driven gear → (4.4) (for the definition of “+” and “-” see Fig. 2.2)
$\xi_{W,k,\pm}(\varphi, \mu)$	real part of $\Xi_{W,k,\pm}(\varphi, \mu)$ → (4.5)
$\Xi_{\rho,k,\pm}(\varphi)$	parametric equation of the parallel curves (fillets) $\Xi_{\rho,k,\pm}$ with distance ρ to curve $\Xi_{M,k,\pm}$ → (4.18)
ρ	fillet radius → Fig. 2.2
ρ^*	factor → (5.7)
φ	rotation angle of the drive gear → Fig. 2.1
$\varphi^*(t)$	rotation angle of the drive gear as time function → (2.4)

$\dot{\varphi}^*(t)$	angular velocity of the drive gear \rightarrow (2.6)
$\varphi_{A,k,+1}$	value of φ with $X_{\varrho,k,+}(\varphi) \cap X_f \neq \emptyset \rightarrow$ (3.31), (7.6), (7.8), (7.9)
$\varphi_{A,k,+2}$	value of φ with $X_{\varrho,k,+}(\varphi) \cap X_{F,k,+} \neq \emptyset \rightarrow$ (7.4) or (5.3), (7.6)
$\varphi_{F,k,+1}$	value of φ with $X_{F,k,+}(\varphi) \cap X_a \neq \emptyset \rightarrow$ (7.5), (7.6)
$\varphi_{F,k,+2}$	value of φ with $X_{F,k,+}(\varphi) \cap X_{\varrho,k,+} \neq \emptyset \rightarrow$ (7.4) or (5.3), (7.6)
$\varphi_{p,k,+1}$	value of φ with $X_a(\varphi) \cap X_{F,k,-} \neq \emptyset \rightarrow$ (7.2), (7.7)
$\varphi_{p,k,+2}$	value of φ with $X_a(\varphi) \cap X_{F,k,+} \neq \emptyset \rightarrow$ (7.5), (7.7)
$\varphi_{A,k,-1}$	value of φ with $X_{\varrho,k,-}(\varphi) \cap X_{F,k,-} \neq \emptyset \rightarrow$ (7.1) or (5.3), (7.3)
$\varphi_{A,k,-2}$	value of φ with $X_{\varrho,k,-}(\varphi) \cap X_f \neq \emptyset \rightarrow$ (7.3), (7.8), (7.9)
$\varphi_{F,k,-1}$	value of φ with $X_{F,k,-}(\varphi) \cap X_{\varrho,k,-} \neq \emptyset \rightarrow$ (7.1) or (5.3), (7.3)
$\varphi_{F,k,-2}$	value of φ with $X_{F,k,-}(\varphi) \cap X_a \neq \emptyset \rightarrow$ (7.2), (7.3)
$\varphi_{S,k,\pm}$	value of φ at the singular point of $X_{F,k,\pm} \rightarrow$ (5.1), (5.2)
$\varphi_{S,\pm}$	value of φ at the singular point of $X_{F,\pm}^*$ (\rightarrow (6.4) and (6.5)) or $\Xi_{F,\pm}^*$ (\rightarrow Theorem 6.2)
$\tilde{\varphi}_{A,k,+1}$	value of φ with $\Xi_{\varrho,k,+}(\varphi) \cap \Xi_{F,k,+} \neq \emptyset \rightarrow$ (7.13) of (5.12), (7.15)
$\tilde{\varphi}_{A,k,+2}$	value of φ with $\Xi_{\varrho,k,+}(\varphi) \cap \Xi_f \neq \emptyset \rightarrow$ (4.19), (7.15)
$\tilde{\varphi}_{F,k,+1}$	value of φ with $\Xi_{F,k,+}(\varphi) \cap \Xi_{\varrho,k,+} \neq \emptyset \rightarrow$ (7.13) or (5.12), (7.15)
$\tilde{\varphi}_{F,k,+2}$	value of φ with $\Xi_{F,k,+}(\varphi) \cap \Xi_a \neq \emptyset \rightarrow$ (7.14), (7.15)
$\tilde{\varphi}_{p,k,+1}$	value of φ with $\Xi_a(\varphi) \cap \Xi_{F,k,-} \neq \emptyset \rightarrow$ (7.11), (7.17), (7.18)
$\tilde{\varphi}_{p,k,+2}$	value of φ with $\Xi_a(\varphi) \cap \Xi_{F,k,+} \neq \emptyset \rightarrow$ (7.14), (7.17), (7.18)
$\tilde{\varphi}_{A,k,-1}$	value of φ with $\Xi_{\varrho,k,-}(\varphi) \cap \Xi_f \neq \emptyset \rightarrow$ (4.19), (7.12), (7.16)
$\tilde{\varphi}_{A,k,-2}$	value of φ with $\Xi_{\varrho,k,-}(\varphi) \cap \Xi_{F,k,-} \neq \emptyset \rightarrow$ (7.10) or (5.12), (7.12)
$\tilde{\varphi}_{F,k,-1}$	value of φ with $\Xi_{F,k,-}(\varphi) \cap \Xi_a \neq \emptyset \rightarrow$ (7.11), (7.12)
$\tilde{\varphi}_{F,k,-2}$	value of φ with $\Xi_{F,k,-}(\varphi) \cap \Xi_{\varrho,k,-} \neq \emptyset \rightarrow$ (7.10) or (5.12), (7.12)
$\tilde{\varphi}_{S,k,\pm}$	value of φ at the singular point of $\Xi_{F,k,\pm} \rightarrow$ (5.10), (5.11)
$\chi(k)$	value of φ in the mid of tooth k , $k = 1, 2, \dots, z_1$ of the drive gear \rightarrow (3.3), value of φ in the mid of tooth space k , $k = 1, 2, \dots, z_2$ of the driven gear
$\psi(\varphi)$	transmission function \rightarrow (2.1), (2.3)
$\psi^*(t)$	rotation angle of the driven gear as time function \rightarrow (2.4)
$\dot{\psi}^*(t)$	angular velocity of the driven gear \rightarrow (2.6)
\bar{A}	conjugate $a - bi$ of the complex number $A = a + bi$
$[A, B]$	exterior product of the complex numbers A and $B \rightarrow$ Appendix A

References

- [1] Bernhard Baule. *Differential- und Integralrechnung*. 9th ed. Vol. 1. Die Mathematik der Naturforscher und Ingenieurs (MNI). Leipzig: S. Hirzel Verlag, 1954.
- [2] Chien-Fa Chen and Chung-Biau Tsay. “Computerized tooth profile generation and analysis of characteristics of elliptical gears with circular-arc teeth”. In: *Journal of Materials Processing Technology* 148 (2004), pp. 226–234.
- [3] DIN 3972. *Bezugsprofile von Verzahnwerkzeugen für Evolventen-Verzahnungen nach DIN 867*. 1952-02.
- [4] Leonhard Euler. “Supplementum de figura dentium rotarum”. In: *Novi commentarii academiae scientiarum Petropolitanae* 11 (1767), 207–231 + 4 tables with figures. URL: [%7Bhttp://eulerarchive.maa.org/%7D](http://eulerarchive.maa.org/%7D).
- [5] Wolfgang Kühnel. *Differentialgeometrie. Kurven - Flächen - Mannigfaltigkeiten*. 6th ed. Springer Spektrum, 2013.

- [6] Bálint Laczik, Peter Zentay, and Richárd Horváth. “A new approach for designing gear profiles using closed complex equations”. In: *Acta Polytechnica Hungarica* 11.6 (2014).
- [7] Faydor L. Litvin and Alfonso Fuentes. *Gear Geometry and Applied Theory*. 2nd ed. Cambridge University Press, 2004.
- [8] Faydor L. Litvin et al. “Design and investigation of gear drives with non-circular gears applied for speed variation and generation of functions”. In: *Comput. Methods Appl. Mech. Engrg.* 197 (2008), pp. 3783–3802.
- [9] Faydor L. Litvin et al. “Generation of planar and helical elliptical gears by application of rack-cutter, hob, and shaper”. In: *Comput. Methods Appl. Mech. Engrg.* 196 (2007), pp. 4321–4336.
- [10] Faydor L. Litvin et al. *Noncircular Gears: Design and Generation*. Cambridge University Press, 2014. ISBN: 9781107683525. URL: <https://books.google.de/books?id=p8MXngEACAAJ>.
- [11] Kurt Luck and Karl-Heinz Modler. *Getriebetechnik – Analyse, Synthese, Optimierung*. (mit 409 Abbildungen einschließlich Konstruktionstafeln und 14 Tafeln). Berlin: Akademie-Verlag, 1990.
- [12] Hans Robert Müller. *Kinematik*. Sammlung Götschen Band 584/584a. Berlin: de Gruyter, 1963.
- [13] Hua Qiu and Gang Deng. “A calculation approach to complete profile of noncircular gear teeth”. In: *Mechatronics and Automatic Control Systems*. Ed. by Wego Wang. Springer-Verlag, 2014.
- [14] Ming-Feng Tsay and Zhang-Hua Fong. “Study of the generalized mathematical model of noncircular gears”. In: *Mathematical and Computer Modelling* 41 (2005), pp. 555–569.
- [15] Walter Wunderlich. *Ebene Kinematik*. Hochschultaschenbuch 447/447a. Mannheim, Wien, Zürich: Bibliographisches Institut, 1970.

English translations of German titles:

- [1] *Differential und integral calculus*
- [3] *Reference profiles for rack-cutters for involute gears according to DIN 867*
- [5] *Differential geometry. Curves - surfaces - manifolds*
- [11] *Design of mechanisms – Analysis, synthesis, optimization*
- [12] *Kinematics*
- [15] *Plane kinematics*

Uwe Bäsel

HTWK Leipzig, University of Applied Sciences,
Faculty of Engineering,
PF 30 11 66, 04251 Leipzig, Germany

uwe.baesel@htwk-leipzig.de